THESIS APPROVAL

GRADUATE SCHOOL, KASETSART UNIVERSITY

Master of Science (Chemistry)
DEGREE

Chemistry
FIELD

Chemistry
DEPARTMENT

TITLE: Structural and Electronic Properties of Methoxy Substituted Cinnamates Based on Quantum Chemical Calculations

NAME: Miss Malinee Promkatkaew

THIS THESIS HAS BEEN ACCEPTED BY

THESIS ADVISOR
(Mr. Songwut Suramitr, Ph.D.)

THESIS CO-ADVISOR
(Associate Professor Supa Hannongbua, Dr.rer.nat.)

THESIS CO-ADVISOR
(Mrs. Thitinun Karpkird, Ph.D.)

DEPARTMENT HEAD
(Assistant Professor Noojaree Prasitpan, Ph.D.)

APPROVED BY THE GRADUATE SCHOOL ON

DEAN
(Associate Professor Gunjana Theeragool, D.Agr.)

THESIS

STRUCTURAL AND ELECTRONIC PROPERTIES OF METHOXY SUBSTITUTED CINNAMATES BASED ON QUANTUM CHEMICAL CALCULATIONS

MALINEE PROMKATKAEW

A Thesis Submitted in Partial Fulfillment of
the Requirements for the Degree of
Master of Science (Chemistry)
Graduate School, Kasetsart University
2009

Malinee Promkatkaew 2009: Structural and Electronic Properties of Methoxy Substituted Cinnamates Based on Quantum Chemical Calculations. Master of Science (Chemistry), Major Field: Chemistry, Department of Chemistry. Thesis Advisor: Mr. Songwut Suramitr, Ph.D. 71 pages.

The structural and electronic properties of methoxy substituted cinnamates with five different substituted positions were investigated using the time-dependent density functional theory (TD-DFT) and symmetry-adapted cluster configuration interaction (SAC-CI) methods. These series included *cis*- and *trans*-isomers of ortho-(**1**), meta-(**2**), and para-(**3**)-monomethoxy and 2,4,5-(**4**) and 2,4,6-(**5**) trimethoxy substituted compounds. The ground state geometries were obtained at the B3LYP/6-31G(d) and B3LYP/6-311G(d) levels of theory, whereas, the excited state geometries were obtained at the CIS/D95(d) levels of theory. All the compounds were stable as *cis*- and *trans*-isomers in the planar structure in both the S_0 and S_1 states, except the 2,4,6-(**5**)-trimethoxy substituted compound. The TD-B3LYP/6-31G(d) and SAC-CI/D95(d) calculations reproduced the recently observed absorption and emission spectra satisfactorily. Three low-lying excited states were found to be relevant for the absorption in the UV blocking energy region. The calculated oscillator strengths of the *trans*-isomers were larger than the respective *cis*-isomers, which is in good agreement with the experimental data. In the ortho- and meta-monomethoxy substituted compounds, the most intense peak was assigned as the transition from next HOMO to LUMO, whereas in the para-monomethoxy substituted compound, it was assigned to the HOMO to LUMO transition. This feature was interpreted as being from the variation of the MOs due to the different substituted positions, and was used to explain the behavior of the excited states of the trimethoxy substituted compounds. The emission from the local minimum in the planar structure was calculated for the *cis*- and *trans*-isomers of the five compounds. The relaxation pathways which lead to the non-radiative decay were also investigated briefly. In the TD-DFT and SAC-CI calculations provide reliable results and a useful insight into the optical properties of these molecules, and therefore, provide a useful tool for developing UVB blocking compounds with regard to the tuning of the absorption.

Student's signature	Thesis Advisor's signature	___ / ___ / ___

ACKNOWLEDGMENTS

I sincerely thank my advisor, Dr. Songwut Suramitr for his considerably helpful comments and tremendous support throughout the duration of my graduate study and research. I also wish to express my appreciation to my advisory committee Associate Professor Dr. Supa Hannongbua, Dr. Thitinun Karpkird, Dr. Supawadee Namuangruk, the representative of Graduate School and also the Co-Advisor of National Nanotechnology Center (NANOTEC) for their worthy suggestion and constructive criticism. Furthermore, special thanks are due to Professor Dr. Masahiro Ehara is also appreciated for his help guidance and valuable suggestions when I did the research at Institute for Molecular Science (IMS), Okazaki, Japan.

I would like to express my deep gratitude to Thailand Graduate Institute of Science and Technology (TGIST) for a scholarship and the Postgraduate Education and Research Program in the National Center of Excellence for Petroleum, Petrochemical Technology and Advance Materials (NCE-PPAM), Thailand Research Fund (TRF), Commission on Higher Education (CHE), Bilateral Research Cooperation (BRC), Faculty of Science, Kasetsart University Research and Development Institute (KURDI), Institute for Molecular Science (IMS) and Graduate School Kasetsart University for partial support, My colleagues at Laboratory for Computational and Applied Chemistry (LCAC) are sincere thanked for their providing helpful assistance and sharing useful ideas and I would also like to thank all of staffs at Department of Chemistry, Faculty of Science, Kasetsart University for research facilities.

Finally, I wish to thanks my family and friends for their advice, encouragement and understanding.

Malinee Promkatkaew
October, 2009

TABLE OF CONTENTS

Page

LIST OF CONTENTS (continued)

Page

LIST OF TABLES

LIST OF TABLES (Continued)

LIST OF FIGURES

Figure **Page**

LIST OF FIGURES (Continued)

LIST OF FIGURES (Continued)

LIST OF ABBREVIATIONS

E_{ex} = Excitation energy
λmax = Maximum wavelength
μ = Dipole moment
$\angle$ = Torsional angle
θ = Rotation angle
AD = Atomic Dipole
B3LYP = Becke's three parameter hybrid functional using the LYP correlation functional
CIS = Singles configuration interaction
D = Debye
DFT = Density Functional Theory
EC = Exchange Correlation
E-OMC = Octyl-*para*-Methoxy-*trans*-Cinnamate
ESF = Electrostatic force
eV = Electron Volt
f = Oscillator strength
GC = Gross Change
HF = Hatree Fock theory
HOMO = Highest Occupied Molecular Orbital
ICT = Intramolecular Charge Transfer
LUMO = Lowest Unoccupied Molecular Orbital
MeOH = Methanol
MOs = Molecular Orbitals
nm = Nanometer
OMC = Octyl-*para*-Methoxy Cinnamate
PCM = Polarized Continuum Model
PM3 = MNDO Parametric Method number3
S_0 = Ground state

LIST OF ABBREVIATIONS (Continued)

S_1 = First excited state

S_2 = Second excited state

S_3 = Third excited state

SAC = Symmetry adapted cluster

SAC-CI = Symmetry adapted cluster-configuration interaction

SD-R = Singles and Doubles-R

TD-DFT = Time-dependent density functional theory

UVR = Ultraviolet radiation

ZINDO = Zerner’s Intermediate Neglect Differential Overlap

Z-OMC = Octyl-*para*-Methoxy-*cis*-Cinnamate

STRUCTURAL AND ELECTRONIC PROPERTIES OF METHOXY SUBSTITUTED CINNAMATES BASED ON QUANTUM CHEMICAL CALCULATIONS

INTRODUCTION

The sun emits a wide spectrum of electromagnetic waves, which ultraviolet radiation (UVR) is the most aggressive towards cellular compounds. Solar UV radiation reaches the earth as well as our skin, is composed of 5-10% highly energetic UVB (290-320 nm) and 90-95% UVA (320-400 nm) which less energetic. The UVB radiation is a directly absorbed by skin surface caused sunburn. Whereas, UVA radiation is more penetrate into deeper skin layer caused suntan, it had been considered to produce less harm than UVB.

As the result, sunscreens were initially developed to protect and minimize all those damaging effects and various photosensitivity and phototoxicity on human skin against UVB radiation. Esters of 4-methoxycinnamic acid are the most popularly have been used as UVB screening compounds in various cosmetic formulations. It has an excellent safety record, is moisturizing, water insoluble, and adheres tenaciously to the skin.

Moreover, cinnamate is one of the interesting arylene system. *Cis-trans* photoisomerization of cinnamate and their derivatives has been the subject of several investigations. However, only few photophysical properties and photoisomerization mechanisms have been studied on experimental and theoretical of cinnamic acid and some unsubstituted cinnamate.

In this work, the structural and electronic properties of the *cis*- and *trans*-isomers of methoxy substituted cinnamates have been theoretically investigated using the time-dependent density functional theory (TD-DFT) and Symmetry-Adapted Cluster Configuration Interaction (SAC-CI) methods. The target molecules were ortho-(**1**), meta-(**2**), and para-(**3**) monomethoxy substituted cinnamates, and 2,4,5-(**4**) and 2,4,6-(**5**) trimethoxy cinnamates, as shown in Figure 1, whose experimental spectra were reported recently. The vertical absorption and emission spectra were calculated at the theoretically optimized molecular geometries. The change in geometry in the first excited state was qualitatively interpreted by using electrostatic force (ESF) theory were performed by Nakatsuji *et al.*, (1973) and (1981). The relaxation paths which lead to the non-radiative decay were also briefly addressed. The difference in electronic transitions among these molecules and the effect of methoxy substitution at the ortho-, meta-, and para-positions were analyzed. In addition, the monomethoxy substituted cinnamates were used for explaining the behavior of trimethoxy substituted cinnamates. The obtained results will lead to the understanding of photophysical properties of UV absorption and emission transition between two isomers that can be used in cosmetics.

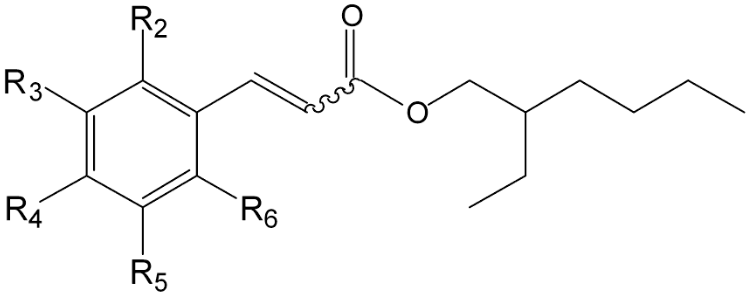

Compounds	R_2	R_3	R_4	R_5	R_6
1	OCH_3	H	H	H	H
2	H	OCH_3	H	H	H
3	H	H	OCH_3	H	H
4	OCH_3	H	OCH_3	OCH_3	H
5	OCH_3	H	OCH_3	H	OCH_3

Figure 1 Chemical structures of cinnamate derivatives.

Source: Karpkird (2009)

LITERATURE REVIEW

Cinnamates have received much attention, as they are the most widely used UVB blocking compounds among the various cosmetic sunscreen agents. Recently, 2-ethylhexyl-4-methoxycinnamate, as well as other cinnamate derivatives, has been developed by Oriol *et al.*, (2003) and Monhapol *et al.*, (2007) as a commercial product. Cinnamates achieve UVB blocking from a ππ* absorption followed by a *cis*–*trans* isomerization at the propenyl double bond in the first excited state (S_1) and a relaxation to the ground state (S_0) involving non-radiative decay, has been investigated by Pattanaargson *et al.*, (2001) and Wang *et al.*, (2007). Pattanaargson *et al.*, (2004) has been studied when exposed to sunlight, this UVB filter will change from octyl-*para*-methoxy-*trans*-cinnamate (*E*-OMC) to octyl-*para*-methoxy-*cis*-cinnamate (*Z*-OMC). The UV absorption spectrum of this UV filter was also shown to be affected by solvents. The study showed a bath chromic shift of the λmax in the UVB region (290-320 nm) from a non-polar solvent to a polar solvent. Although no other degradation product was detected when *E*-OMC was exposed to sunlight except the configurationally isomer *Z*-OMC, the UVB filtering efficiency was shown to be decreased.

As a UVB blocking compound, the optical properties, in particular the photoabsorption efficiency in the UVB energy region is an important factor. In order to achieve the favorable optical properties, molecular design using the variation of the substituents has been extensively performed. The photochemistry of the process and the involvement of a intramolecular charge transfer (ICT) state resulting from a rotation at the C=C double bond has also been studied by Singh *et al.,* (2008) and Chakraborty *et al.,* (2006). Smith *et al.,* (1998) shown that diethyl ether enhance photoisomerisation by competing with and thereby disrupting, the hydrogen bonding between cinnamic acid and other polyene carboxylic acid molecules which impedes rotation about their double bonds. Photoisomerisation is reversible and, after a period of exposure to UV radiation, a photostationary, *cis*-*trans* equilibrium is attained. As the UVB absorbance of the *cis*-isomer is less than that of the *trans*-isomer. For example, Huong *et al.,* (2007) and Pattanaargson *et al.,* (2004) investigated the photoisomerization of the sun filter ethylhexyl-*para*-methoxycinnamate (OMC) was studied under various concentrations in various solvents was measured. The result indicates that equilibrium of photoisomerization depends upon concentration and polarity of the solvent used. To explain these special spectral behaviors, the quantum chemical calculations were performed by Yang *et al.,* (2008) investigated that the ground state and excited state molecular geometries, electronic structure, absorption and emission properties.

Several experimental and theoretical studies have been conducted to elucidate the optical properties and photochemistry of cinnamates. Singh *et al.,* (2008) has been utilized to investigate the photochemistry of *trans*-ethyl-*para*-(dimethylamino) cinnamate by examining the twist coordinates by using time-dependent density functional theory (TD-DFT), corroborating the experimental observation that the formation of an intramolecular charge transfer state is feasible in the excited state. Recently, the photophysical properties of methoxy substituted cinnamates, i.e., ortho-, meta-, and para-monomethoxy cinnamates and 2,4,5- and 2,4,6-trimethoxy 2-ethylhexyl-cinnamates, have been investigated experimentally to develop better UVB filter compounds are shown as Karpkird *et al.,* (2009). The excited states and spectroscopic properties of *para*-hydroxy cinnamate were investigated using TD-DFT and CASSCF methods by Groot de M. *et al.,* (2009). Pattanaargson *et al.,* (2004) and Smith *et al.,* (1998) were also observed that the UV absorption and fluorescence are affected by the solvent, with a shift to longer wavelengths in polar solvents. These studies have provided some useful insights into the optical properties of these molecules. However, reliable theoretical work is still necessary to understand the details of the optical properties of these molecules, such as the difference in the absorption and emission of the *cis*- and *trans*-isomers and the effect of the solvent.

In the quantum chemical calculations are carried out in order to determine the energy required for configurationally changes. The calculated reaction path between different structures and the localization of the transition state exhibit a high photosensitivity in the visible or the near infrared spectrum for this ester and related in different positions of the aromatic group. The optimized structure obtained for the configurations reveal a planar molecular system about the conjugated π system. In 2005 and 2007, Suramitr and coworker investigated the torsional energy curves for the carbazole-based molecules by partial optimization, based on the B3LYP method. The torsional angle (ω) is defined as $\omega = 0°$ corresponds to the *cis*-isomer and $\omega = 180°$ corresponds to the *trans*-isomer. All stationary points located on the torsional energy were characterized as minima by harmonic frequency calculation for minimum energy structures all frequencies are real and symmetrical torsional angle synchronously.

Jacquemin *et al., (*2007) found that the low-lying excited states using the time dependent density functional theory (TD-DFT) have been the subject of an intense study and a detailed understanding of its photochemistry. TD-DFT methodology allowing excited state optimizations with the inclusion of bulk solvent effects has been proposed and applied compare gas-phase and solvent effect. In addition, the wavelengths of absorption and emission have been compared to the available experimental values. Yang *et al.*, (2008) and Meeto *et* al., (2008) shown that TD-DFT was used for the vertical excitation energies and absorption properties calculation and the optimized geometry in the ground state was employed to perform this vertical TD calculation. The compounds were performed by single point calculations at the optimized geometries of the ground state. The excitation energy, based on the first and second singlet-singlet electronic transitions were studied. The implicit assumption underlying this approximation is that the lowest singly excited state can be described by only one singly excited configuration in which an electron is promoted from the Highest Occupied Molecular Orbital (HOMO) to the Lowest Unoccupied Molecular Orbital (LUMO) are given in Suramitr *et al.*, (2005 and 2007).

The symmetry-adapted cluster configuration interaction (SAC-CI) method was developed by Nakatsuji and coworkers to obtain a detailed interpretation and prediction of the molecular spectroscopy and photochemistry of the molecules. The SAC-CI method has been established by Nakatsuji (1992) and Ehara *et al.*, (2005) as a reliable and useful method for investigating a wide variety of chemical phenomena through many successful applications. The method has been utilized for the accurate theoretical spectroscopy of many π-conjugated systems by Nakatsuji *et al.,* (1985) and Wan *et al.,* (2000). Nakatsuji *et al.,* (1996, 1998 and 2007) and Fujimoto *et al.,* (2005) have also been applied to the photochemistry of biological systems, such as porphyrins, photosynthetic reaction centers, retinal, and luciferin. Recently, the photophysical properties and excited state dynamics of fluorescent molecules, such as fluorine-thiophene oligomers and poly(*para*-phenylene-vinylene) and poly(*para*-phenylene) that are useful for organic light-emitting diodes were investigated and the absorption/emission spectra of these molecules were elucidated by Poolmee *et al.,* (2005) and Saha *et al.,* (2007). These works confirm that the SAC-CI method is useful for investigating the electronic excitations and excited state dynamics of large π-conjugated systems.

METHOD OF CALCULATIONS

1. Model setup

The molecular structure of the *cis*- and *trans*-isomers of methoxy substituted ortho-(**1**), meta-(**2**), para-(**3**) monomethoxy substituted cinnamates and 2,4,5-(**4**) and 2,4,6-(**5**) trimethoxy substituted cinnamates is shown in Figure 1. In this work, the structural and electronic properties of the cinnamate compounds are shown in Figure 2(a) were investigated using the TD-DFT methods. Whereas, the model compounds are shown in Figure 2(b) were investigated using the SAC-CI method by modifying the hydrocarbon side chain to methyl group. To reduce the computational requirements without sacrificing the essence of the excitation, as the electronic structure relevant to the photophysical properties can be described using this molecular structure.

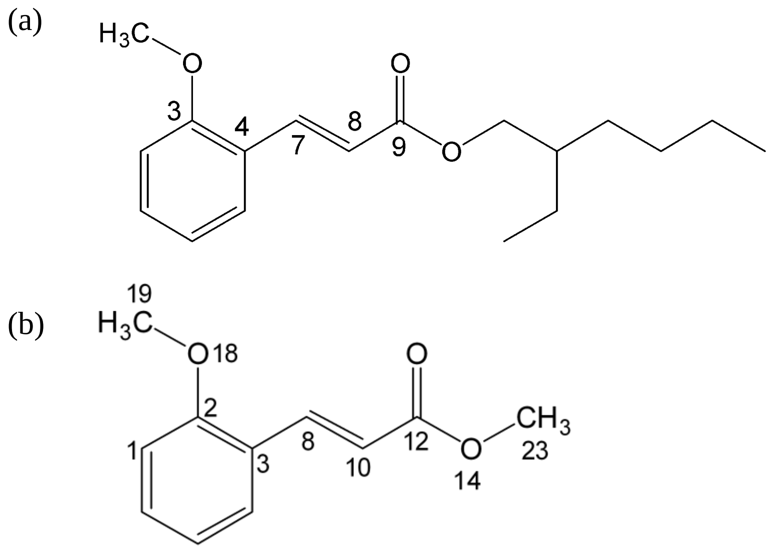

Figure 2 Molecular structures and atom numbering of the *trans*-1 compounds for the (a) TD-DFT and (b) SAC-CI calculations.

2. Geometrical optimization

The molecular structure of the *cis*- and *trans*-isomers of methoxy substituted ortho-(**1**), meta-(**2**), para-(**3**) monomethoxy cinnamates and 2,4,5-(**4**) and 2,4,6-(**5**) trimethoxy cinnamates were investigated based on the time-dependent density functional theory (TD-DFT) and symmetry-adapted cluster configuration interaction (SAC-CI) methods.

In the TD-DFT calculations, the ground state (S_0) geometries were fully optimized without restricting the symmetry using the B3LYP/6-31G(d) method along the torsional angle ($\angle C_4$-C_7-C_8-C_9) are shown in Figure 2(a). Whereas, the SAC-CI calculations, the ground state (S_0) geometries were fully optimized without restricting the symmetry using the B3LYP /6-311G(d) method along the torsional angle ($\angle C_3$-C_8-C_{10}-C_{12}). In addition, to investigate the energy barrier of the model compound for the rotation of the methoxy group which affects the optical properties, the ground state potential energy curves along the rotation (θ) of the methoxy group with respect to the phenyl ring ($\angle C_1$-C_2-O_{18}-C_{19}) were calculated using the B3LYP/6-311G(d) method are shown in Figure 2(b).

The potential energy curve of the ortho-(**1**), meta-(**2**), and para-(**3**) monomethoxy substituted cinnamates, and 2,4,5-(**4**) and 2,4,6-(**5**) trimethoxy cinnamates were investigated by partial optimization, based on the B3LYP/6-31G(d) method. Each point on the potential energy curve of the ground state was obtained as a function of the torsional angle $\angle C_3$-C_4-C_7-C_8 by fixing $\angle C_3$-C_4-C_7-C_8 and its symmetrical torsional angle synchronously, at 30° intervals, between 0° and 180° and optimizing all other parameters.

To calculate the emission energy, the geometry optimization was performed for the first singlet excited (S_1) states using the CIS/D95(d) method with restricting the planar structure, except for the *cis*-**5** compound. The emission from this local minimum was observed in previous experimental work, although the global minimum exists in the nonplanar structure where the torsional angle of the $\angle C_3\text{-}C_8\text{-}C_{10}\text{-}C_{12}$ chain is around 90°.

3. Electronic properties

The absorption energies were calculated using the TD-DFT and SAC-CI methods. In the TD-DFT calculations, the vertical excitation energies were calculated for the optimized geometries of the ground state with the B3LYP/6-31G(d) method. The effects of solvent inclusion were analyzed by comparisons between gas-phase and methanol solution systems by the polarized continuum model (PCM). Whereas, the SAC-CI calculations, the vertical excitation energies were calculated for the optimized geometries of the ground state with the double-zeta basis set of the Huzinaga and Dunning plus polarization function (D95(d)).

The emission energies were calculated using the SAC-CI method with the D95(d) basis sets. The SAC-CI calculations based on the CIS optimized structure have been validated in many applications for photofunctional molecules and biological compounds.

To reduce the computational requirement, the singles and doubles (SD)-*R* method with the direct calculation of the σ-vector, i.e., the direct SAC-CI approach was used. The perturbation selection technique was used to reduce the computational cost and a Level-Two accuracy was adopted. The threshold of the linked terms for the ground state was set to $\lambda_g = 5.0 \times 10^{-6}$. All the product terms generated by the doubles were included in the SAC calculations. For the excited states, the threshold of the linked doubles were set to $\lambda_e = 5.0 \times 10^{-7}$. All the product terms generated by the R_1S_2 and R_2S_2 operators were included in the SAC-CI calculations.

All calculations were performed using the Gaussian03 suite of programs whereas, the SAC/SAC-CI calculations with modifications for executing the direct SAC-CI method.

RESULTS AND DISCUSSION

1. TD-DFT calculations

1.1 Molecular geometries

The molecular structure of the *cis*- and *trans*-isomers of the *cis*- and *trans*-isomers of methoxy substituted ortho-(**1**), meta-(**2**), para-(**3**) monomethoxy cinnamates and 2,4,5-(**4**) and 2,4,6-(**5**) trimethoxy cinnamates are shown in Figure 3. As the results, all compounds are stable at *cis*- and *trans*-isomers and the torsional angle ($\angle C_3$-C_4-C_7-C_8) locates around 0^o and 180^o, respectively, are displayed in Table 1. All the compounds, except for the *cis-5* structure has been distorted by the steric interaction of methoxy group substitution at ortho-position (R_2 and R_6) are displayed in Figure 4.

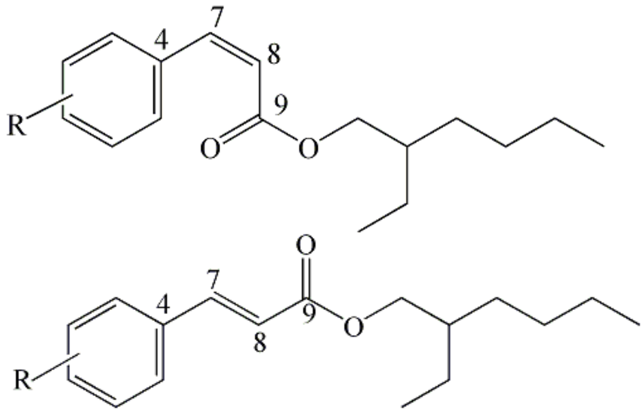

Figure 3 Molecular structure of *cis*-(top) and *trans*-(bottom)-isomers of cinnamate derivatives with atom numbering.

Table 1 Ground state bond length (Å) for *cis*- and *trans*-isomer of methoxy substituted cinnamate were optimized at ground state by the B3LYP/6-31G(d) level of theory.

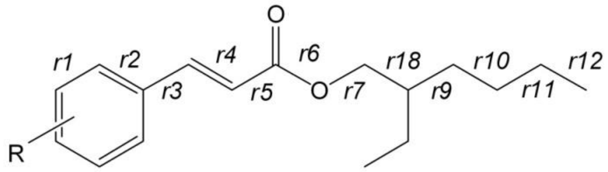

	cis-isomer					*trans*-isomer				
Parameters	**1**	**2**	**3**	**4**	**5**	**1**	**2**	**3**	**4**	**5**
Bond lengths										
r1	1.398	1.398	1.383	1.400	1.391	1.400	1.401	1.394	1.403	1.391
r2	1.428	1.406	1.416	1.418	1.418	1.421	1.400	1.404	1.411	1.427
r3	1.462	1.467	1.460	1.454	1.465	1.461	1.464	1.458	1.455	1.454
r4	1.358	1.355	1.358	1.361	1.350	1.347	1.345	1.347	1.350	1.352
r5	1.473	1.475	1.471	1.469	1.474	1.475	1.477	1.474	1.471	1.473
r6	1.361	1.360	1.361	1.363	1.366	1.359	1.357	1.358	1.362	1.364
r7	1.441	1.442	1.441	1.439	1.438	1.441	1.443	1.441	1.440	1.438
r8	1.530	1.529	1.530	1.530	1.531	1.530	1.529	1.530	1.530	1.530
r9	1.553	1.553	1.553	1.553	1.552	1.553	1.553	1.552	1.553	1.553
r10	1.536	1.536	1.536	1.536	1.536	1.536	1.536	1.536	1.536	1.536
r11	1.534	1.534	1.534	1.534	1.534	1.534	1.534	1.534	1.534	1.534
r12	1.532	1.532	1.532	1.532	1.532	1.532	1.532	1.532	1.532	1.532
Torsional angle ($\angle C_3$-C_4-C_7-C_8)	-0.5	0.0	-0.2	0.5	7.1	179.6	179.8	179.6	180.0	179.8

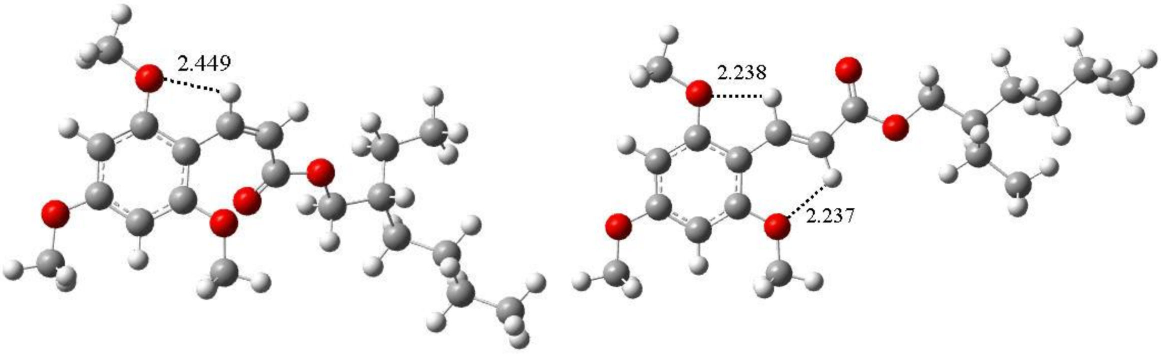

Figure 4 Intra-molecular hydrogen bonding interaction of *cis*-**5** *(*left) and *trans*-**5** (right)-isomers of cinnamate derivatives.

1.2 Conformational analysis

The molecular structure of the *cis*- and *trans*-isomers of the *cis*- and *trans*-isomers of methoxy substituted ortho-(**1**), meta-(**2**), para-(**3**) monomethoxy substituted cinnamates and 2,4,5-(**4**) and 2,4,6-(**5**) trimethoxy substituted cinnamates were examined for the torsional angle ($\angle C_3\text{-}C_4\text{-}O_7\text{-}C_8$) from 0 to 180° in steps of 30°. The potential energy curves for this rotation of 5 compounds are shown in Figure 5. It was found that the torsional angle ($\angle C_3\text{-}C_4\text{-}O_7\text{-}C_8$) as 0° are corresponding to *cis*-isomer and the torsional angle ($\angle C_3\text{-}C_4\text{-}O_7\text{-}C_8$) as 180° are corresponding to the *trans*-isomer. At the torsional angle of 90^{o}, the energy barrier to the perpendicular conformation for ortho-(**1**), meta-(**2**), para-(**3**), 2,4,5-(**4**) and 2,4,6-(**5**) compounds was 6.27, 5.72, 6.89, 7.26 and 7.49 kcal/mol, respectively. Therefore, the torsional energy barrier of the 2,4,5-(**4**) and 2,4,6-(**5**) compounds are higher than the para-(**3**), ortho-(**1**), and meta-(**2**) compounds. This shows that the ortho-(**1**), 2,4,5-(**4**) and 2,4,6-(**5**) compounds have intramolecular C-H···O hydrogen bond interaction between the oxygen atom of the methoxy group and the hydrogen atom in the vinylene group .

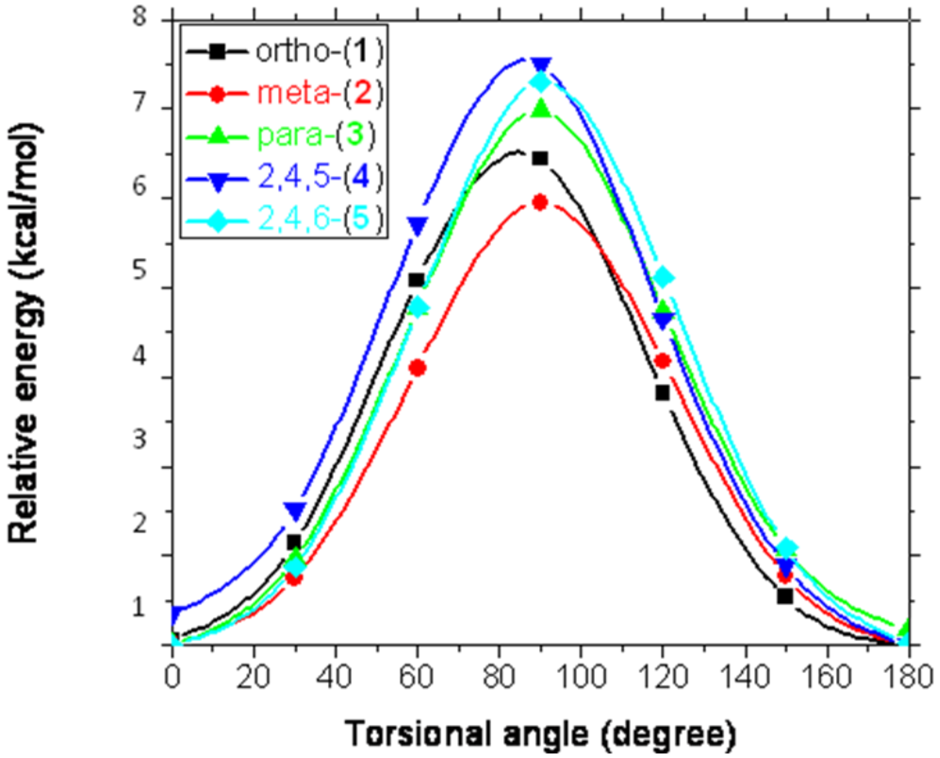

Figure 5 Ground state potential energy curves along the torsional angle ($\angle C_3$-C_4-O_7-C_8) of methoxy substituted cinnamates obtained by using the B3LYP/6-31G(d) method.

1.3 TD-DFT absorption spectra

The vertical excitation energies (E_{ex}) were performed by single point calculations at the optimized geometries of the ground state by the TD-B3LYP/6-31G(d) methods. In the Table 2, there are three low-lying excited states to be relevant in the energy region of the UV absorption. For the gas phase, the mono-substituted methoxycinnamates are ortho-(*cis*-**1** and *trans*-**1**), meta- (*cis*-**2** and *trans*-**2**) and para-(*cis*-**3** and *trans*-**3**) found that the largest transition probabilities of ortho- and meta-positions are the transition from the ground state to the third excited state ($S_0 \rightarrow S_3$) and main electronic transitions are corresponding to next HOMO excite to LUMO. Whereas, the largest transition possibilities of para-position is the transition from the ground state to the first excited state ($S_0 \rightarrow S_1$) and corresponding to the electronic excitation from HOMO to LUMO.

In Table 3, trimethoxy substituted at ortho-, meta- and para-positions (*cis*-**4** and *trans*-**4**) give the largest transition from ground state to first excited state ($S_0 \rightarrow S_1$). The main electronic transition is corresponded to HOMO excite to LUMO, as same as the compounds which have only substituted at ortho and para position (*cis*-**5** and *trans*-**5**). It is indicated that the para-methoxy substitution is an important effect to electronic properties of cinnamate derivatives, based on Figure 6.

Table 2 Excitation energy (E_{ex}), absorption wavelength (λ_{max}) and oscillator strength (*f*) of gas phase and solvent effect for the *cis*-and *trans*-isomers of monomethoxy substituted cinnamates calculated using the TD/B3LYP/6-31G(d) level of theory.

Molecule	Excited	Gas phase			Solvent effect			Excitation	Experiment(nm)	
	state	E_{ex} (eV)	λmax(nm)	*f*	E_{ex} (eV)	λmax(nm)	*f*	character	MeOH	Hexane
cis-**1**	$S_0 \rightarrow S_1$	3.86	321	0.28	3.71	334	0.35	0.60 (H → L)	313	
	$S_0 \rightarrow S_2$	4.28	290	0.00	4.32	287	0.38	0.68 (H-2 → L)		
	$S_0 \rightarrow S_3$	4.43	280	0.39	4.39	283	0.01	0.59 (nH → L)	271	274
trans-**1**	$S_0 \rightarrow S_1$	3.97	313	0.36	3.77	329	0.41	0.60 (H → L)	325	
	$S_0 \rightarrow S_2$	4.35	285	0.00	4.41	281	0.45	0.68 (H-2 → L)		
	$S_0 \rightarrow S_3$	4.59	270	0.42	4.60	269	0.01	0.59 (nH → L)	276	272
cis-**2**	$S_0 \rightarrow S_1$	3.76	330	0.04	3.73	332	0.05	0.65 (H → L)	313	
	$S_0 \rightarrow S_2$	4.31	288	0.00	4.36	284	0.75	0.69 (H-2 → L)		
	$S_0 \rightarrow S_3$	4.49	276	0.66	4.42	280	0.01	0.61 (nH → L)	274	271
trans-**2**	$S_0 \rightarrow S_1$	3.97	312	0.06	3.83	324	0.09	0.62 (H → L)	313	
	$S_0 \rightarrow S_2$	4.38	283	0.00	4.42	281	0.84	0.68 (H-2 → L)		
	$S_0 \rightarrow S_3$	4.59	270	0.75	4.61	269	0.00	0.57 (nH → L)	278	274
cis-**3**	$S_0 \rightarrow S_1$	4.05	306	0.68	3.91	317	0.76	0.70 (H → L)	303	296
	$S_0 \rightarrow S_2$	4.37	284	0.00	4.49	276	0.00	0.70 (H-2 → L)		
	$S_0 \rightarrow S_3$	4.56	272	0.01	4.54	273	0.01	0.61 (nH → L)		
trans-**3**	$S_0 \rightarrow S_1$	4.20	295	0.91	3.99	311	1.01	0.63 (H → L)	309	290
	$S_0 \rightarrow S_2$	4.43	280	0.00	4.60	269	0.00	0.68 (H-2 → L)		
	$S_0 \rightarrow S_3$	4.66	266	0.02	4.68	265	0.00	0.51 (nH → L)		

Table 3 Excitation energy (E_{ex}), absorption wavelength (λ_{max}) and oscillator strength (*f*) of gas phase and solvent effect for the *cis*- and *trans*-isomers of trimethoxy substituted cinnamates calculated using the TD/B3LYP/6-31G(d) level of theory.

Molecule	Excited	Gas phase			Solvent effect			Excitation	Experiment(nm)	
	state	E_{ex} (eV)	λmax(nm)	*f*	E_{ex} (eV)	λmax(nm)	*f*	character	MeOH	Hexane
cis-**4**	$S_0 \rightarrow S_1$	3.37	368	0.33	3.30	376	0.43	0.68 (H → L)	345	349
	$S_0 \rightarrow S_2$	4.28	290	0.39	4.21	295	0.38	0.67 (nH → L)		
	$S_0 \rightarrow S_3$	4.40	282	0.00	4.46	278	0.00	0.69 (H-2 → L)		
trans-**4**	$S_0 \rightarrow S_1$	3.59	345	0.47	3.40	365	0.54	0.68 (H → L)	349	348
	$S_0 \rightarrow S_2$	4.42	280	0.00	4.30	288	0.44	0.69 (H-2 → L)		
	$S_0 \rightarrow S_3$	4.47	278	0.43	4.65	267	0.00	0.65 (nH → L)		
cis-**5**	$S_0 \rightarrow S_1$	3.82	325	0.30	3.70	335	0.35	0.64 (H → L)	305	298
	$S_0 \rightarrow S_2$	4.11	302	0.05	3.99	310	0.06	0.67 (nH → L)		
	$S_0 \rightarrow S_3$	4.52	274	0.03	4.61	269	0.02	0.67 (H-2 → L)		
trans-**5**	$S_0 \rightarrow S_1$	4.12	301	0.85	3.90	318	0.94	0.62 (H → L)	320	312
	$S_0 \rightarrow S_2$	4.26	291	0.03	4.02	308	0.04	0.65 (nH → L)		
	$S_0 \rightarrow S_3$	4.45	278	0.00	4.70	264	0.00	0.68 (H-2 → L)		

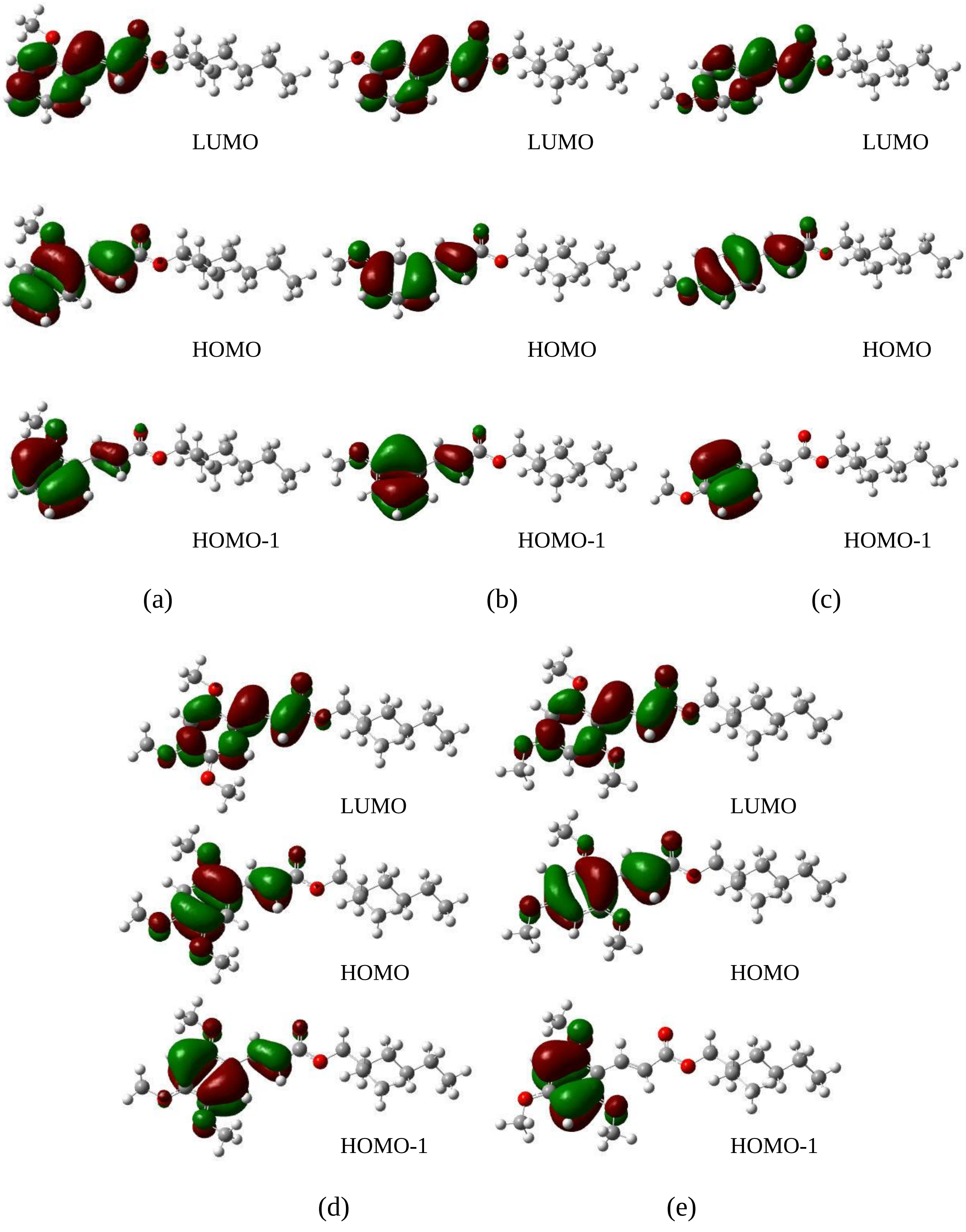

Figure 6 MOs relevant to the low-lying excited states for: (a) *trans*-**1**, (b) *trans*-**2**,(c) *trans*-**3**, (d) *trans*-**4** and (e) *trans*-**5** of methoxy substituted cinnamates calculated by using the TD-B3LYP/6-31G(d) method.

1.4 Solvent effect

For the effects of solvent, all compounds were analyzed by the polarized continuum model (PCM) in methanol solution systems by using the TD-B3LYP/6-31G(d) methods (Table 2 and 3). The PCM model calculates the molecular free energy in solution as the sum over three terms: electrostatic, dispersion-repulsion and cavitation energy. All three terms are calculated using a cavity defined through interlocking *van der Waals*-spheres centered at atomic positions. As the results, the excitation energies of solvent effect shift to the longer wavelengths than the experiment results. Because of the PCM methods is the simple method to analyzed solvent effect in Gaussian03.

Comparison of the oscillator strengths between gas phase and solvent effect for all the compounds found that the influence of the methanol solution lead to increases absorption wavelengths. While, the oscillator strengths in gas phase agree well with the experimental data in UVB absorption spectrum are displayed in Figure 7 and Figure 8.

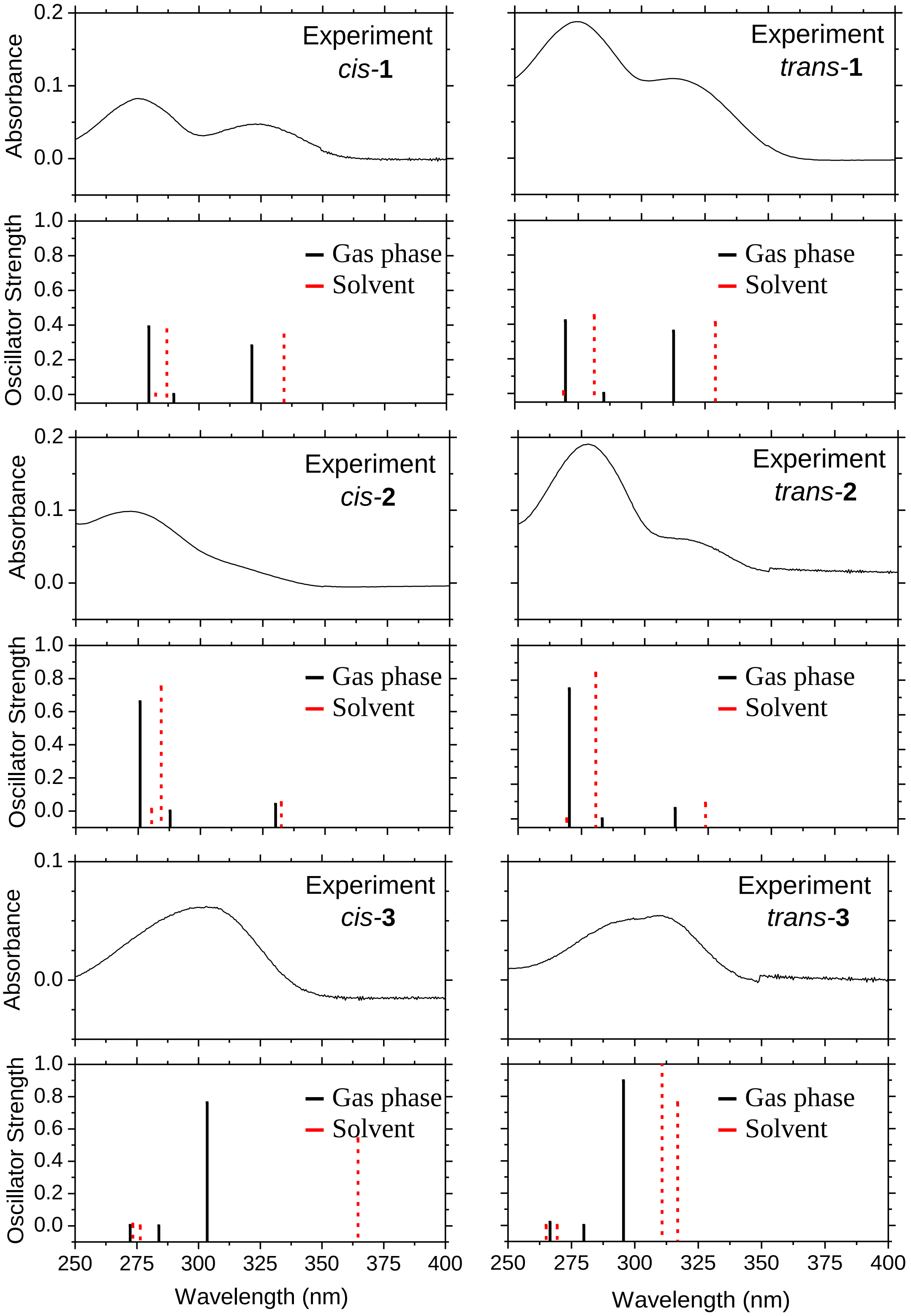

Figure 7 TD-DFT absorption spectra of the *cis*- and *trans*-isomers of the mono-methoxy compounds compared with the experimental spectrum in methanol.

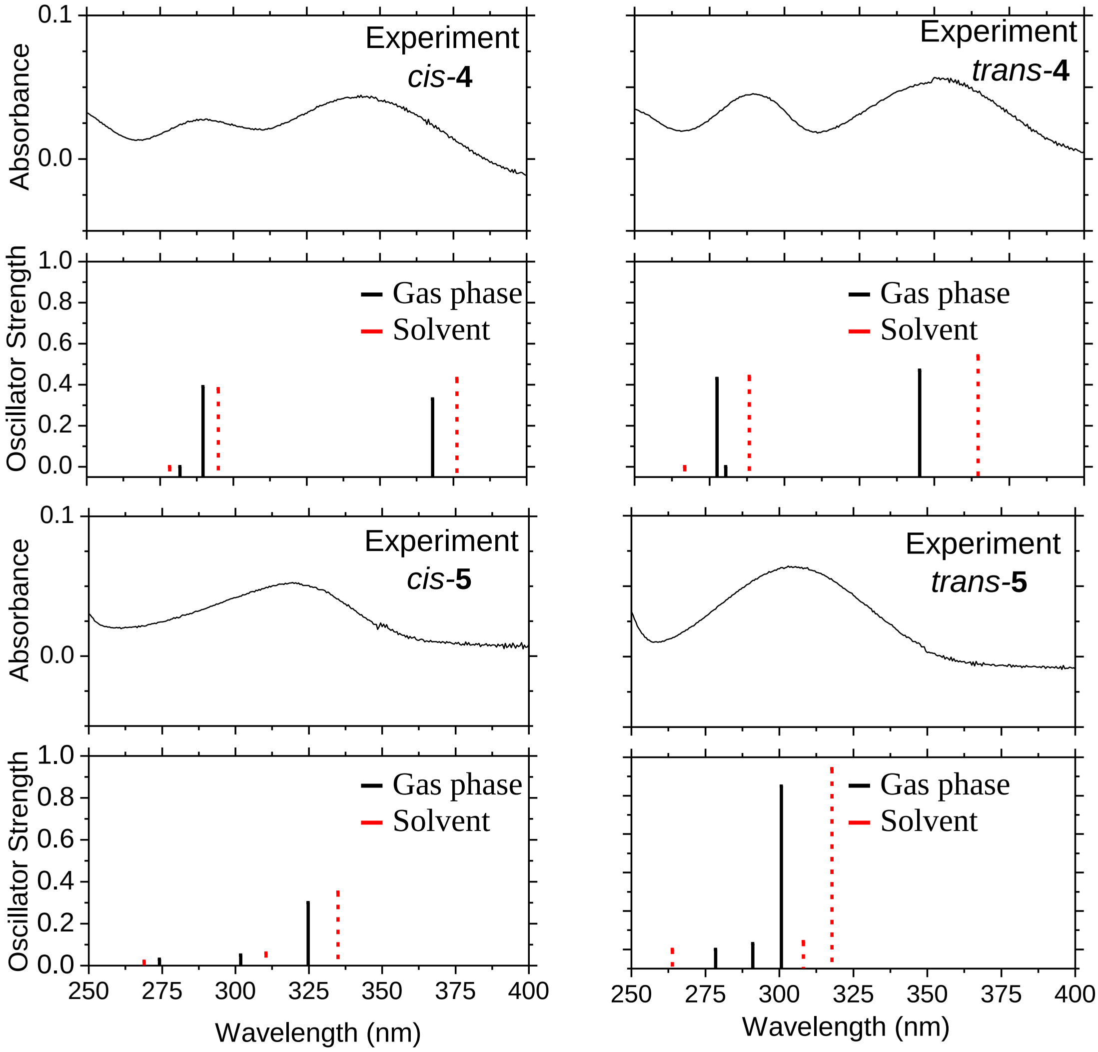

Figure 8 TD-DFT absorption spectra of the *cis*- and *trans*-isomers of the trimethoxy compounds compared with the experimental spectrum in methanol.

2. SAC-CI calculations

2.1 Structural properties

2.1.1 Ground state and excited state geometries

The ground (S_0) and first excited (S_1) state geometries of the *cis*- and *trans*-isomers of ortho-(**1**), meta-(**2**), para-(**3**) and the 2,4,5-(**4**) and 2,4,6-(**5**) methoxy substituted compounds were investigated by B3LYP/6-311G(d) and CIS/D95(d) methods, respectively. The molecular geometries were fully optimized both of the S_0 and S_1 state without restricting the symmetry along the torsional angle ($\angle C_3$-C_8-C_{10}-C_{12}). The model structure and atomic numbering of 10 compounds are displayed in Figure 9. The bond length results of the *trans*-isomers are shown in Table 4, and those of the *cis*-isomers are given in Table 5. All the compounds, except for the *cis*-**5** compound, had local minima in the coplanar structure of the *cis*- and *trans*-isomers in both the S_0 and S_1 states due to π-conjugation. As shown later, in the S_0 state, the rotational energy barrier of the methoxy group is very low, although the planar structure is the most stable structure.

In the S_1 state, the global minima are in the form of a nonplanar structure, but local minima exist in the planar structure. The emission was observed from this local minimum in the planar structure, and in particular, a strong emission was observed for compound **2**. The lifetime was also measured for all the compounds with regard to this emission. A characteristic molecule is the *cis*-**5** compound, which has a stable nonplanar structure with the torsional angle as 7.6° in the S_0 state because of steric effects. A local minimum of the *cis*-**5** compound in the S_1 state could not be obtained.

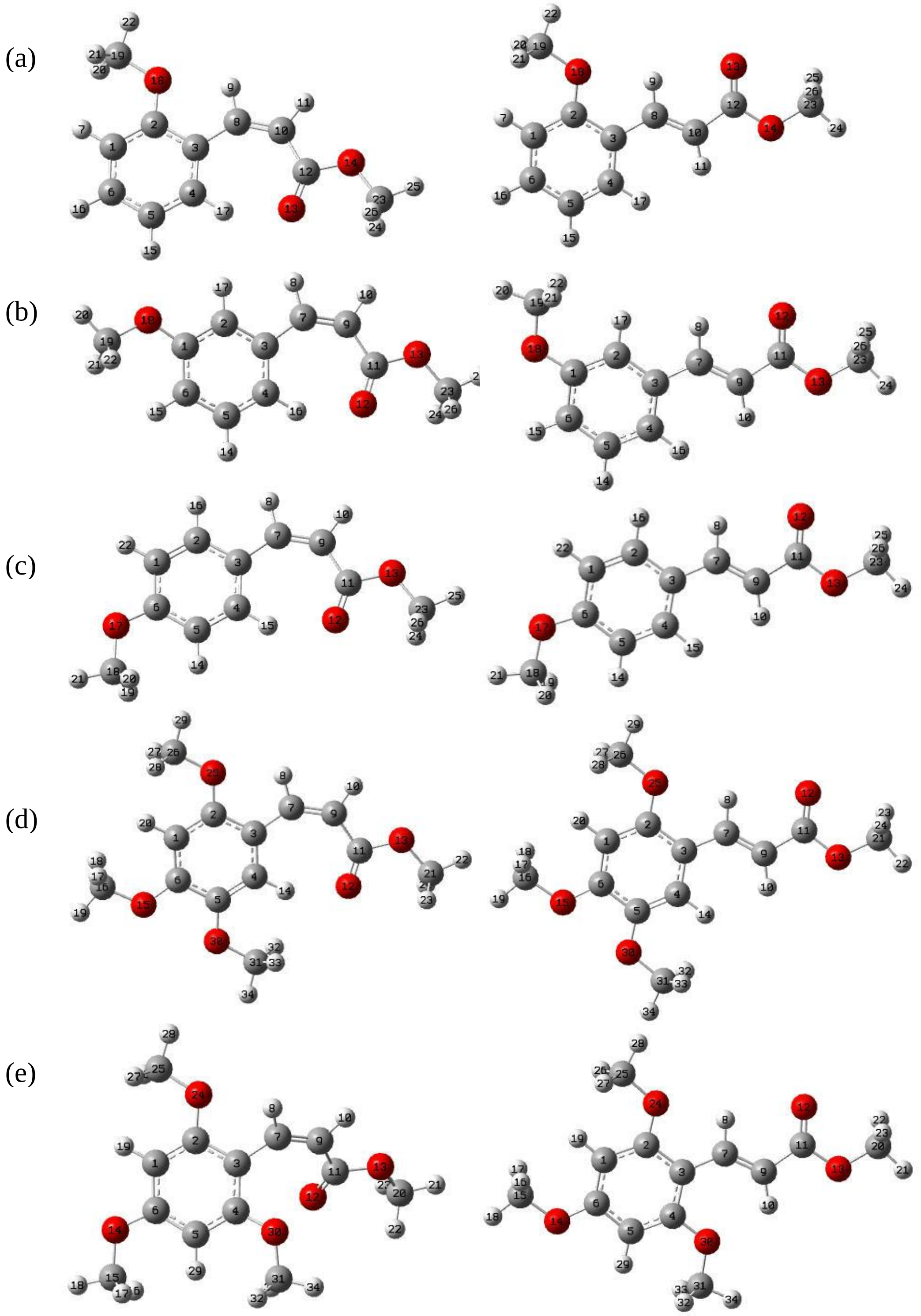

Figure 9 Model structure and atom numbering of *cis*-(left) and *trans*-(right)-isomers of (a) ortho-(**1**) (b) meta-(**2**) (c) para-(**3**) (d) 2,4,5-(**4**) and (e) 2,4,6-(**5**)-methoxy substitution calculated by using the SAC-CI method.

Table 4 Ground state (S_0) and lowest singlet excited state (S_1) geometries of *trans*-isomers of methoxy substitution calculated by using B3LYP/6-311G(d) and CIS/D95(d) methods, respectively.

	trans-**1**		*trans*-**2**		*trans*-**3**		*trans*-**4**		*trans*-**5**	
Parameters	S_0	S_1	S_0	S_1	S_0	S_1	S_0	S_1	S_0	S_1
Bond lengths										
$r(C_1\text{-}C_2)$	1.398	1.376	1.395	1.366	1.383	1.353	1.401	1.373	1.398	1.372
$r(C_2\text{-}C_3)$	1.419	1.467	1.407	1.432	1.408	1.443	1.408	1.464	1.418	1.464
$r(C_3\text{-}C_8)$	1.460	1.400	1.463	1.403	1.458	1.400	1.453	1.407	1.452	1.402
$r(C_8\text{-}C_{10})$	1.343	1.400	1.342	1.397	1.344	1.400	1.346	1.392	1.348	1.448
$r(C_{10}\text{-}C_{12})$	1.474	1.456	1.475	1.457	1.473	1.454	1.470	1.392	1.471	1.411
$r(C_{12}\text{-}O_{14})$	1.358	1.336	1.355	1.335	1.358	1.337	1.361	1.340	1.363	1.343
$r(O_{14}\text{-}C_{23})$	1.433	1.414	1.434	1.414	1.434	1.414	1.342	1.412	1.431	1.411
Torsional angle($\angle C_3\text{-}C_8\text{-}C_{10}\text{-}C_{12}$)	180.0	180.0	180.0	180.0	180.0	180.0	180.0	180.0	180.0	180.0

Table 5 Ground state (S_0) and lowest singlet excited state (S_1) geometries of *cis*-isomers of methoxy substitution calculated by using B3LYP/6-311G(d) and CIS/D95(d) methods, respectively.

	cis-**1**		*cis*-**2**		*cis*-**3**		*cis*-**4**		*cis*-**5**
Parameters	S_0	S_1	S_0	S_1	S_0	S_1	S_0	S_1	S_0
Bond lengths									
$r(C_1\text{-}C_2)$	1.395	1.376	1.396	1.372	1.381	1.354	1.398	1.375	1.389
$r(C_2\text{-}C_3)$	1.426	1.480	1.403	1.424	1.414	1.448	1.416	1.473	1.415
$r(C_3\text{-}C_8)$	1.460	1.406	1.466	1.409	1.459	1.406	1.452	1.413	1.464
$r(C_8\text{-}C_{10})$	1.354	1.409	1.351	1.404	1.354	1.412	1.358	1.402	1.346
$r(C_{10}\text{-}C_{12})$	1.471	1.456	1.474	1.455	1.469	1.452	1.467	1.451	1.473
$r(C_{12}\text{-}O_{14})$	1.360	1.342	1.359	1.340	1.360	1.343	1.362	1.344	1.365
$r(O_{14}\text{-}C_{23})$	1.432	1.412	1.433	1.412	1.433	1.412	1.431	1.410	1.430
Torsional angle($\angle C_3\text{-}C_8\text{-}C_{10}\text{-}C_{12}$)	0.0	0.0	0.0	0.0	0.0	0.0	0.0	0.0	7.6

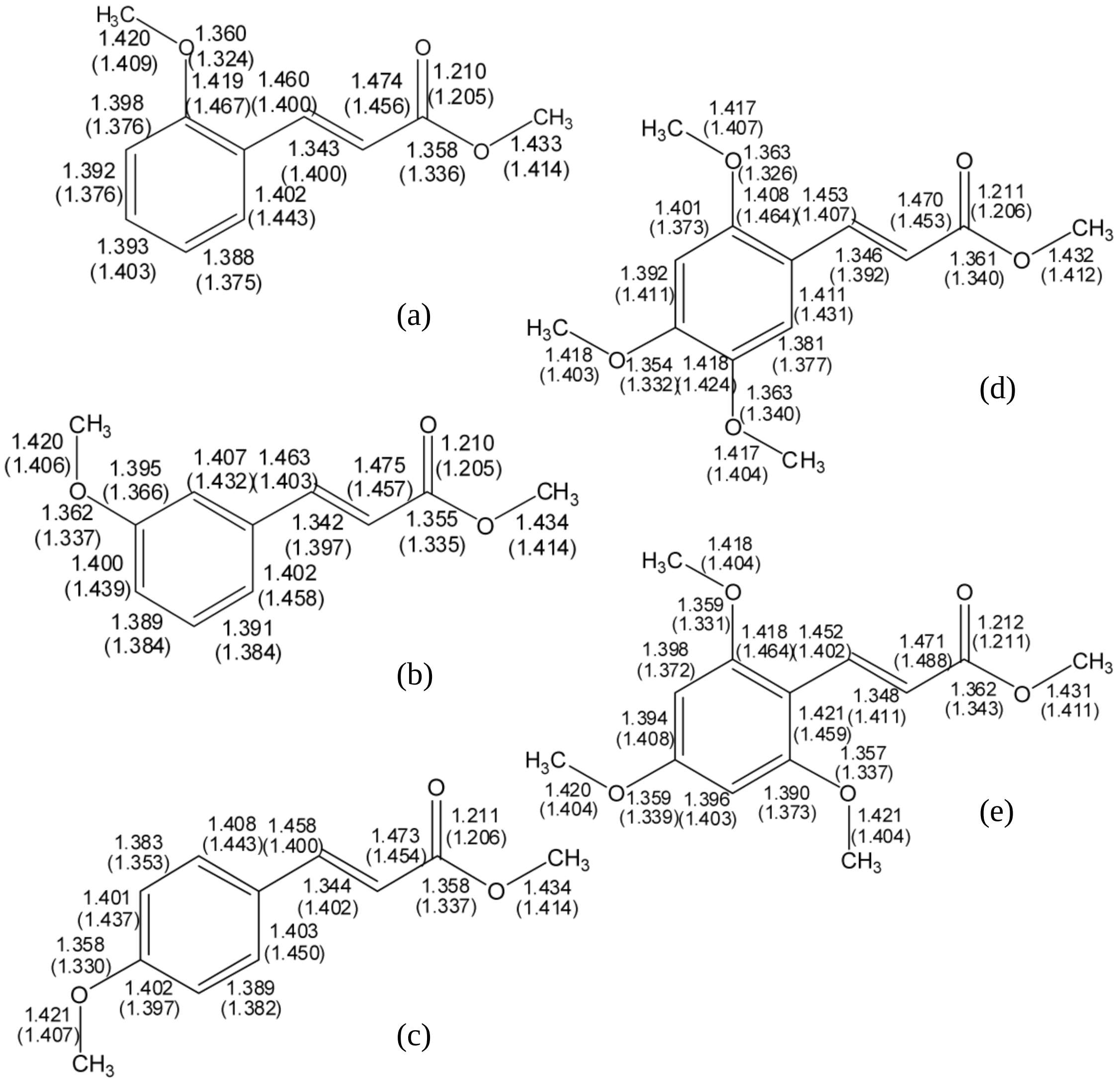

Figure 10 A comparison of the changes in *C–C* and *C–O* bond lengths along the conjugation between the ground state and the first singlet excited state (in parentheses) of: (a) *trans*-**1**, (b) *trans*-**2**, (c) *trans*-**3**, (d) *trans*-**4**, and (e) *trans*-**5** calculated by using the B3LYP/6-311G(d) and CIS/D95(d) methods, respectively.

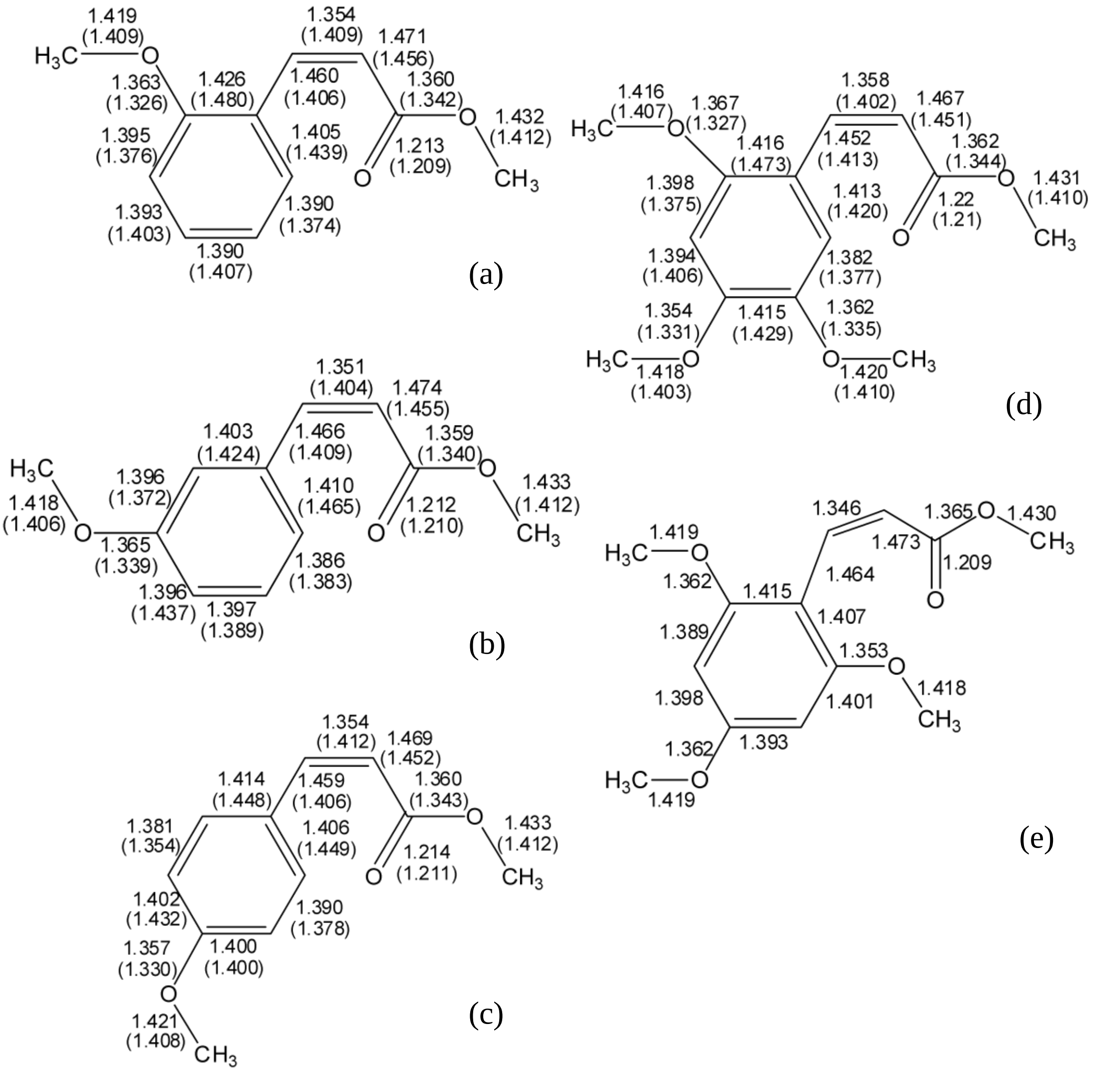

Figure 11 A comparison of the changes in *C–C* and *C–O* bond lengths along the conjugation between the ground state and the first singlet excited state (in parentheses) of: (a) *cis*-**1**, (b) *cis*-**2**, (c) *cis*-**3**, (d) *cis*-**4**, and (e) *cis*-**5** calculated by using the B3LYP/6-311G(d) and CIS/D95(d) methods, respectively.

A comparison of the *C*-*C* and *C*-*O* bond lengths along the conjugation between the S_0 and S_1 state geometries of the *trans*-isomers of the methoxy substituted compounds is shown in Figure 10, and those of the *cis*-isomers are given in Figure 11. It was found that the C_1-C_2, C_3-C_8, C_{10}-C_{12}, C_{12}-O_{14}, and O_{14}-C_{23} bond lengths decrease and the length of the other bonds increases. In the S_0 state, the *C*-*C* bond alternation exists for both the single and double bonds, but this bond alternation relaxes in the S_1 state. Since the excitation is relatively localized in the central unit, the prominent changes occur in the vinylene unit. For example, in the *trans*-**1** compound, the change in bond length is Δr = +0.048, –0.060, and +0.057 Å for C_2-C_3, C_3-C_8, and C_8-C_{10}, respectively, while the other changes in bond length are within 0.022 Å.

2.1.2 Geometry relaxation in excited state

The geometry change in the excited state could be qualitatively interpreted using ESF theory. We analyzed the geometry relaxation in the S_1 state of the *trans*-**3** molecule is displayed in Figure 12. Based on ESF theory, the geometry change in the excited state is caused by the force acting on the nuclei due to the change in electron distribution. The molecular geometry is determined by balancing the atomic dipole (AD), exchange (EC), and gross charge (GC) forces. The difference in the SAC/SAC-CI electron density between the S_0 and S_1 states in the ground state geometry is shown in Figure 8. The EC force of the *C*=*C* bond decreases because of the decrease in electron density, while the EC force enhances the *C*–*C* bond. For example, the C_1-C_2, C_3-C_8, C_{10}-C_{12}, C_{12}-O_{14}, and O_{14}-C_{23} bonds shrink where the electron density increases (blue) and the C_2-C_3 and C_8-C_{10} bonds become longer where the electron density decreases (yellow). Geometry relaxation of other molecules can also be explained in the same manner.

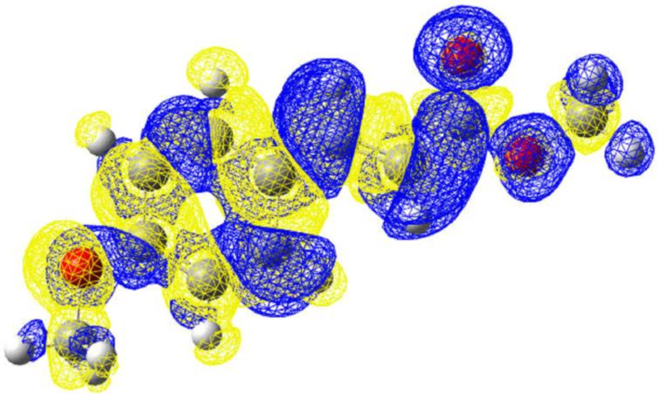

Figure 12 Density difference maps of the *trans*-**3** of methoxy substituted molecules with a positive diffuse (blue) and a negative diffuse (yellow).

2.1.3 Potential energy curves along torsion

The rotation of the methoxy group relative to the plane of the phenyl ring was investigated. The ortho-(*trans*-**1**), meta-(*trans*-**2**) and the para-(*trans*-**3**) substituted compound were examined for the C_1-C_2-O_{18}-C_{19} angle from 0 to 90° in steps of 15°. We calculated the potential energy curves with freezing other coordinates and estimated the energy barrier. The potential energy curves for this rotation are shown in Figure 13, and these indicate that the most stable conformation was located at a angle of $\theta = 0°$ for the *trans*-**1**, *trans*-**2** and *trans*-**3** compounds. At the rotation angle of 90°, the energy barrier to the perpendicular conformation of the methoxy group for the *trans*-**1**, *trans*-**2** and *trans*-**3** compounds was 2.8, 3.2 and 3.6 kcal/mol, respectively.

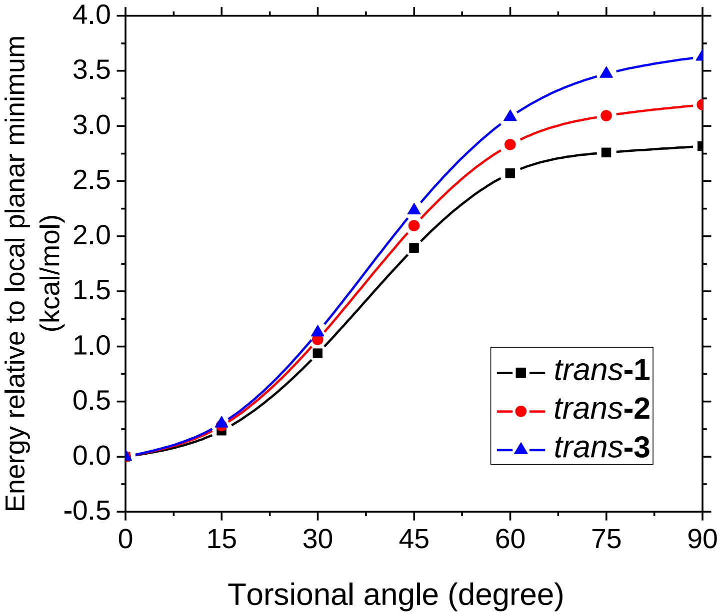

Figure 13 Ground state potential energy curves along the rotation of the methoxy group (θ) for the *trans*-**1** and *trans*-**3** compounds calculated by using the B3LYP/6-311G(d) method.

This shows that the π-conjugation of the *trans*-**3** compound is slightly more effective than that of the *trans*-**1** and *trans*-**2** compounds in the planar structure.The extent of π-conjugation between the methoxy oxygen and the phenyl ring could be reflected in the *C-O* bond length; when the bond is shorter, the conjugation is more effective. In the trans compounds, the *C-O* bond lengths are 1.360, 1.362, and 1.358 Å, for *trans*-**1**, *trans*-**2** and *trans*-**3** compounds, respectively. In *trans*-**1**, the intramolecular C–H···O hydrogen bond interaction between the oxygen atom of the methoxy group and the hydrogen atom in the vinylene group also exists in the *trans*-**1** compound, which causes a reverse effect on the energy barrier. This low rotational energy barrier of about 1.0 kcal/mol from θ = 0–30° indicates that a wide range of nonplanar conformations is possible at room temperature. The effect of the nonplanar structure on the absorption spectra will be discussed later.

The ground state potential energy curve is flat along the rotation angle θ = 0-30°, where the energy difference is less than 1.0 kcal/mol, and therefore, the nonplanar conformation contributes to the absorption spectra at room temperature. Therefore, we calculated the SAC-CI absorption spectra of the *trans*-**1** and *trans*-**3** compounds in the nonplanar structure. The calculated spectra with a rotation angle of θ = 0, 15, and 30° are shown in Figure 14. For the *trans*-**1** compound**,** the lower energy peak shows a blue shift of about 10 nm from θ = 0 to 30° and this contributes to the shoulder observed in the higher energy region. Since the HOMO of the *trans*-**1** compound has an anti-phase interaction between the benzene ring and the methoxy group, the HOMO stabilizes the nonplanar structure, and therefore, the blue shift occurs in the S_1 state of the H-L transition. The oscillator strength of the *trans*-**1** compound in the S_2 and S_3 states also interchanges along the rotation. The S_3 state is strong at θ = 0°, while in the distorted structure, the oscillator strength of the S_2 state increases. On the other hand, the oscillator strength of the three excited states of the *trans*-**3** compound does not change much.

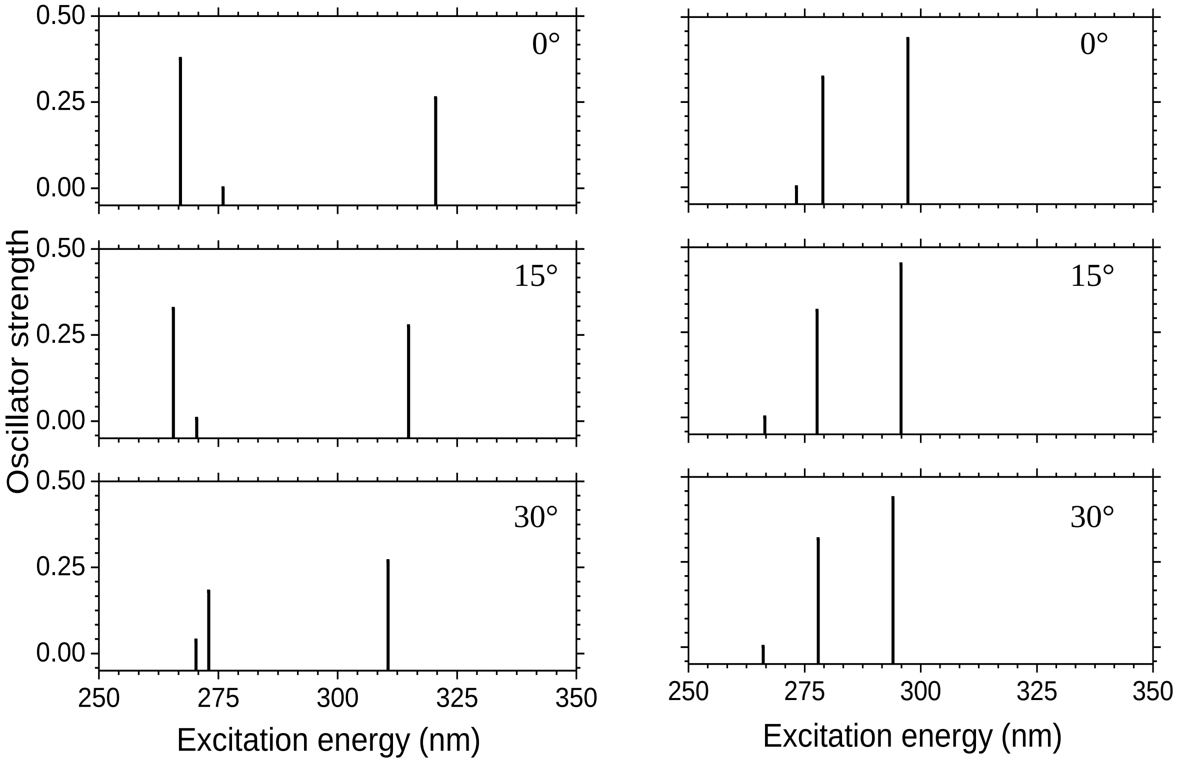

Figure 14 Absorption spectra of the *trans*-**1** (left) and *trans*-**3** (right) compounds at a torsional angle θ = 0°, 15°, and 30° calculated by using the SAC-CI/D95(d) method.

2.2 Electronic properties

2.2.1 SAC-CI absorption spectra

The absorption spectra of the *cis*- and *trans*-isomers of the five methoxy substituted cinnamates were investigated. The vertical excitation energies were calculated using the SAC-CI/D95(d) method in their ground state optimized structure. The calculated excitation energies, oscillator strength, and dipole moments are summarized in Table 6 and Table 7, along with the experimental values observed in hexane and methanol. The A' states were assigned to the ππ* excited states with a large oscillator strength, while the A'' states were due to the nπ* transition. Three low-lying excited states were found to be relevant in the energy region of the UV absorption. The higher excited states were also examined, up to around 7 eV, but as these states are located above 5 eV, they do not contribute to the important energy region for UVB absorption of 290-320 nm (4.28-3.87 eV). Compound **3** is the standard commercial product for UVB protection.

For the monomethoxy substituted compounds, the excited states that contribute to the absorption have a different character that depends on the methoxy substituted position. In the case of the ortho-(*cis*-**1** and *trans*-**1**) and meta-(*cis*-**2** and *trans*-**2**) compounds, the S_3 state has the highest transition probability, and is characterized as being the transition from the next HOMO to LUMO (nH-L) transition, whereas, the highest transition possibility of the para- (*cis*-**3** and *trans*-**3**) compounds was calculated for the $S_0 \rightarrow S_1$ transition, and the excitation character is a HOMO-LUMO (H-L) transition.

Table 6 Excitation energy (E_{ex}), absorption wavelength (λ_{max}), oscillator strength (f), excitation character and dipole moment for the *cis*- and *trans*-isomers of monomethoxy substituted cinnamates calculated by using the SAC-CI/D95(d) level of theory.

Molecule	State	E_{ex} (eV)	λ_{max}(nm)	f		Dipole moment (D)		Experiment(nm)	
					Excitation character	$\lvert\mu\rvert$[a]	$\lvert\Delta\mu\rvert$[b]	MeOH	Hexane
cis-**1**	*XA'*					2.44			
	1A'	3.83	323	0.25	0.77 (H →L)	6.49	1.68	313	
	1A''	4.49	276	0.00	0.78 (H-3→L)	2.05	1.75		
	2A'	4.51	275	0.34	0.72 (nH →L)	2.54	0.10	271	274
trans-**1**	*XA'*					2.78			
	1A'	3.87	321	0.26	0.77 (H →L)	5.75	1.25	325	
	1A''	4.23	293	0.00	0.82 (H-3→L)	3.24	2.35		
	2A'	4.64	267	0.38	0.71 (nH →L)	2.75	0.10	276	272
cis-**2**	*XA'*					1.09			
	1A'	3.94	314	0.04	0.76 (H →L)	6.65	2.19	313	
	1A''	4.26	291	0.00	0.82 (H-3→L)	3.56	1.71		
	2A'	4.74	261	0.53	0.73 (nH →L)	3.99	1.14	274	271
trans-**2**	*XA'*					0.50			
	1A'	4.06	306	0.12	0.69 (H →L)	5.31	1.92	313	
	1A''	4.49	276	0.00	0.80 (H-3→L)	5.42	2.32		
	2A'	4.61	269	0.47	0.62 (nH →L)	2.92	0.98	278	274
cis-**3**	*XA'*					0.80			
	1A'	4.13	300	0.59	0.91 (H →L)	4.54	1.58	303	296
	1A''	4.33	286	0.00	0.83 (H-3→L)	4.46	1.68		
	2A'	4.41	281	0.04	0.71 (H →nL)	1.27	0.20		

[a] Values in parentheses show the difference of the dipole moments between the ground and excited states ($\lvert\vec{\mu}_{ES}\rvert - \lvert\vec{\mu}_{GS}\rvert$).

[b] Values show the changes of the dipole moments from the ground state to excited state ($\lvert\Delta\vec{\mu}\rvert = \lvert\vec{\mu}_{ES} - \vec{\mu}_{GS}\rvert$).

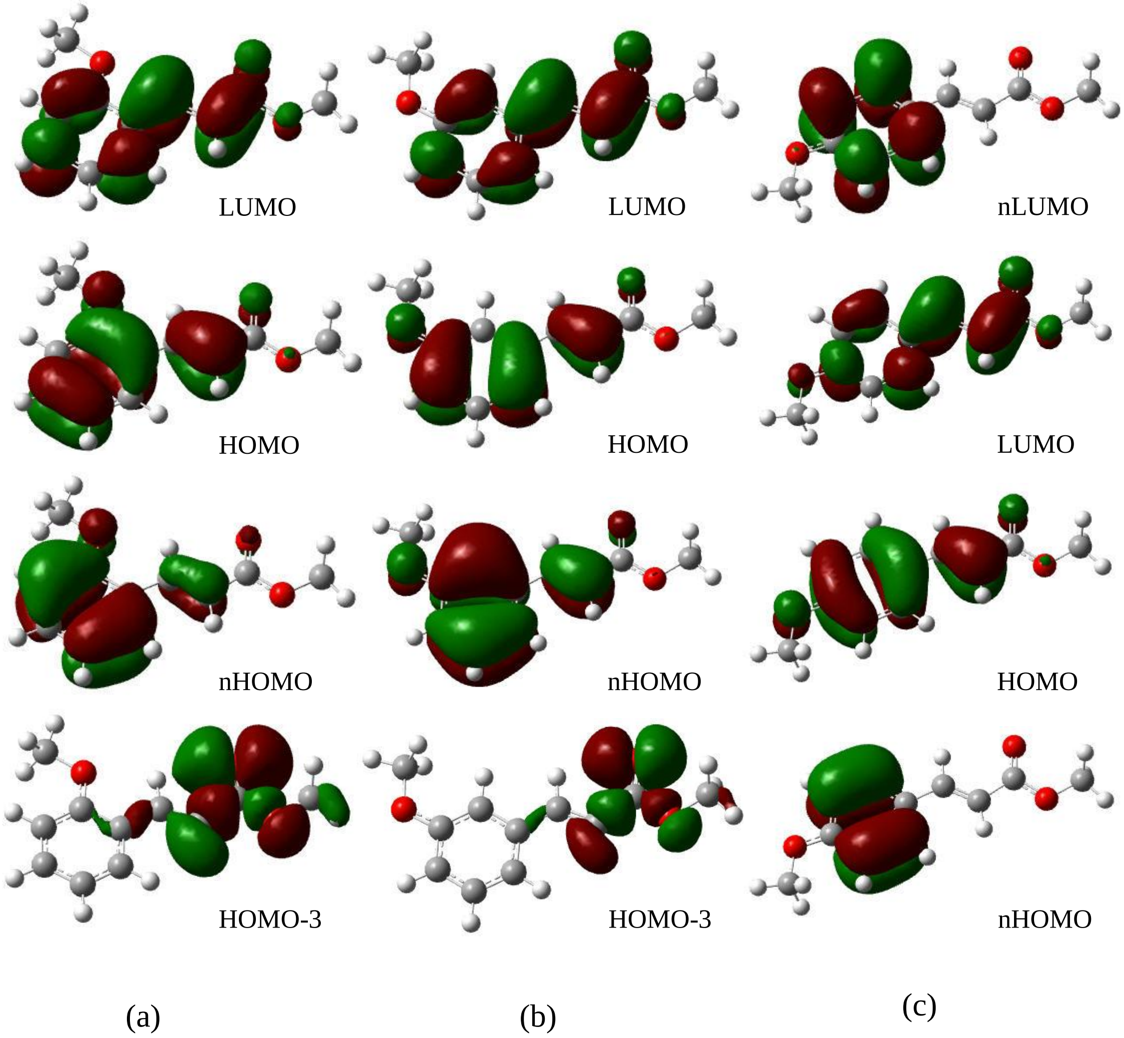

Figure 15 MOs relevant to the low-lying excited states for: (a) ortho-(*trans*-**1**), (b) meta-(*trans*-**2**), and (c) para-(*trans*-**3**) methoxy substituted molecules.

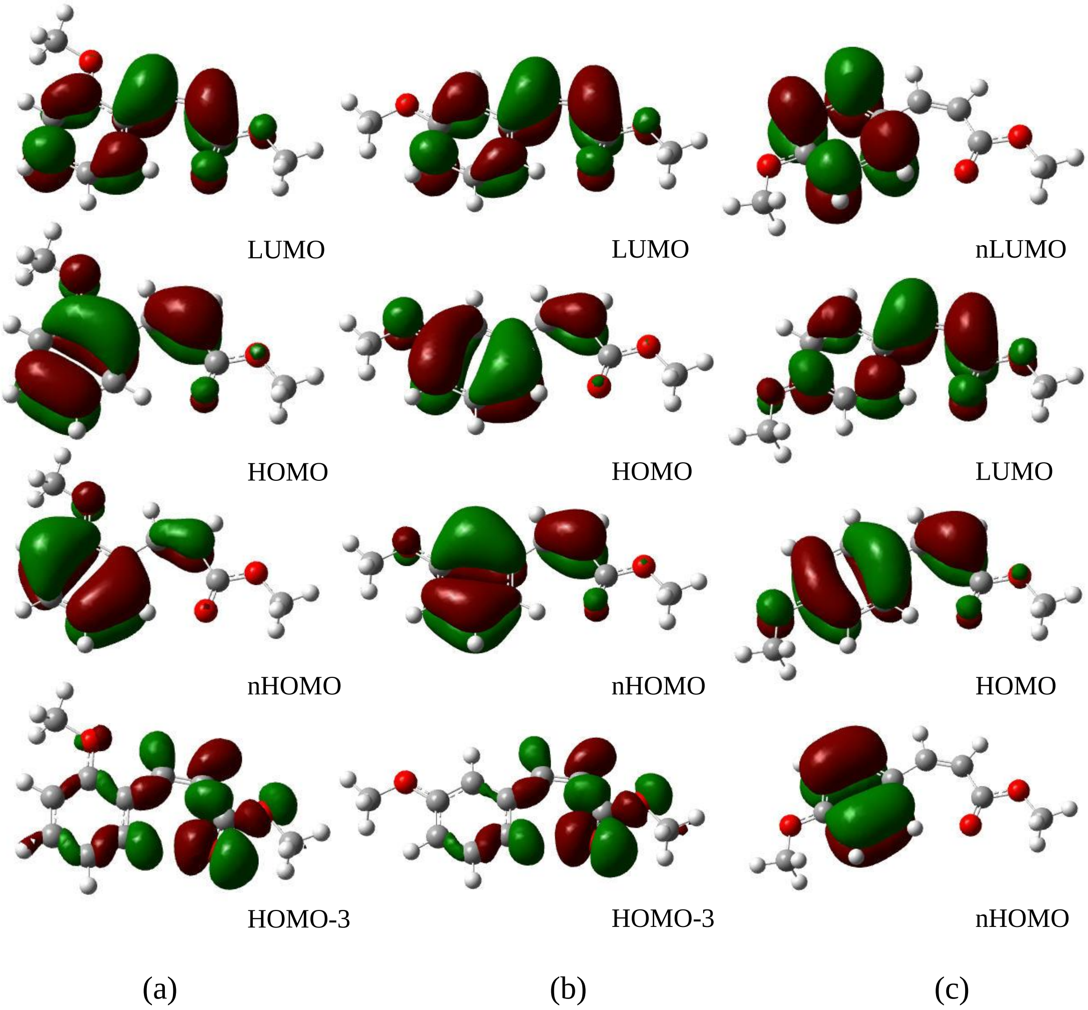

Figure 16 MOs relevant to the low-lying excited states for: (a) ortho-(*cis*-**1**), (b) meta-(*cis*-**2**), and (c) para-(*cis*-**3**) of the methoxy substituted molecules.

The agreement with the experimental values was satisfactory. The deviations from the experimental values in peak position were within about 10 nm. For example, for the *cis*-**2** compound, the calculated values were 261 and 314 nm, compared with the experimental values of 274 (271) and 313 nm, respectively. For the transition probability, the observed absorption coefficients of the *trans*-**1** compound are 13,500 and 18,100 $M^{-1}cm^{-1}$ for the lower and higher peaks, respectively, and the calculated oscillator strengths are 0.26 and 0.38 for these peaks, respectively.

The deviation from the experimental data can be attributed to the solvent effect and/or our model neglecting the side chain. The polar solvent effect is relatively small for compounds **1** and **2**, as the difference in the experimental excitation energy between hexane and methanol solutions is within 4 nm, while it is large for compound **3**, at 7–19 nm.[7] The dipole moments of the ground and excited states were calculated to interpret the solvent effect qualitatively. The calculated dipole moments of the excited state were larger than that of the ground state, which causes a red shift of the peaks in a polar solvent. We also calculated the absolute values of the changes of the dipole moments from the ground state to excited states, $|\Delta\vec{\mu}| = |\vec{\mu}_{ES} - \vec{\mu}_{GS}|$, which are shown in Table 1, to examine the solvent effect before the solvent reorientation due to the excitation of cinnamates. The *cis*-isomers of compounds **1** and **2** showed differences in their dipole moments between the ground and excited states of 0.10 and 2.89 debye ($|\Delta\vec{\mu}|$ are 0.10 and 1.14 debye), respectively, whereas the difference in dipole moment of compound **3** was around 3.74 debye ($|\Delta\vec{\mu}|$ is 1.58 debye), which also explains the observed experimental trend. However, our calculations for compounds **4** and **5** could not explain the experimental data. The *cis*- and *trans*-isomers of compound **4** show a large difference in their dipole moments, around 4.71 and 4.38 debye ($|\Delta\vec{\mu}|$ are 2.23 and 1.72 debye), compared with the energy shift of only 4 and 1 nm, respectively. This may be explained by the direct interaction between methanol and cinnamates.

The trimethoxy substituted compounds at the ortho-, meta-, and para-positions (*cis*-**4** and *trans*-**4**) show two separate peaks, and the strong lowest absorption occurs around 350 nm. However, this lowest peak is below the UVB region of interest. The *trans*-**5** compound has the S_1 state at 307 nm with a large oscillator strength of 0.64. However, this value is lower than that of the *trans*-**3** compound of 0.76 (S_1 + S_2). Experimental data also show the same trend. The absorption coefficients were 24,700 and 19,900 $M^{-1}cm^{-1}$ in methanol for the *trans*-**3** and *trans*-**5** compounds, respectively.[7] The *1A′* and *2A′* states were characterized as being H–L and nH–L transitions, respectively, for both compounds **4** and **5**. The para-methoxy substitution has an important effect in achieving a large oscillator strength of H-L transition in cinnamates. Methoxy substitution in the meta position leads to a decrease in the oscillator strength of the H-L transition as also seen in compound **2**. A comparison with the absorption spectrum of methyl hydroxycinnamate (pCA)[8] in the gas phase shows that the substitution of methoxy for OH results in changes in the oscillator strengths of the S_1 and S_2 transitions. The oscillator strength of the H-nL transition increases in methoxy substituted compound: the TD-DFT calculation predicted that the S_2 state has smaller oscillator strength in hydroxy cinammate.

Table 7 Excitation energy (E_{ex}), absorption wavelength (λ_{max}), oscillator strength (f), excitation character and dipole moment for the *cis*- and *trans*-isomers of trimethoxy substituted cinnamates calculated by using the SAC-CI/D95(d) level of theory.

Molecule	State	E_{ex} (eV)	λ_{max}(nm)	f		Dipole moment (D)		Experiment (nm)	
					Excitation character	$\|\mu\|$[a]	$\|\Delta\mu\|$[b]	MeOH	Hexane
cis-**4**	*XA'*					3.02			
	1A'	3.33	372	0.36	0.89 (H →L)	7.73	2.23	345	349
	1A''	4.30	288	0.00	0.82 (H-3→L)	1.62	1.78		
	2A'	4.34	286	0.24	0.77 (nH →L)	3.82	0.67		
trans-**4**	*XA'*					3.14			
	1A'	3.45	360	0.41	0.88 (H →L)	7.52	1.72	349	348
	2A'	4.48	277	0.30	0.73 (nH →L)	4.95	0.77		
	1A''	4.52	274	0.00	0.79 (H-3→L)	3.35	2.46		
cis-**5**	*XA'*					2.26			
	1A	4.09	303	0.24	0.83 (H →L)	6.96	1.92	305	298
	2A	4.35	285	0.01	0.71 (nH →L)	4.02	0.73		
	3A	4.56	272	0.11	0.70 (H-4→L)	4.04	0.79		
trans-**5**	*XA'*					5.04			
	1A'	4.04	307	0.64	0.88 (H →L)	5.62	0.29	320	312
	2A'	4.27	290	0.06	0.74 (nH →L)	6.93	0.78		
	1A''	4.57	271	0.00	0.79 (H-3→L)	1.32	2.31		

[a] Values in parentheses show the difference of the dipole moments between the ground and excited states ($|\vec{\mu}_{ES}| - |\vec{\mu}_{GS}|$).

[b] Values show the changes of the dipole moments from the ground state to excited state ($|\Delta\vec{\mu}| = |\vec{\mu}_{ES} - \vec{\mu}_{GS}|$).

Figure 15 shows the MOs relevant for the three low-lying excited states for the *trans*-**1**, *trans*-**2**, and *trans*-**3** compounds. The corresponding MOs for the *cis*-**1**, *cis*-**2**, *cis*-**3** compounds and compounds **4** and **5** are shown in Figures 16 and 17. The patterns of the MOs of the *cis* form are similar to those of the *trans* one. The HOMO, next HOMO, and LUMO are localized on the phenylene vinylene backbone. The methoxy substitution on the phenyl ring also has a small contribution to the π-conjugation. HOMO-3 contains the lone pairs of the C=O bond, and the nπ* transition ($1A''$ state) causes a charge transfer from the C=O bond to the phenylene vinylene. In the HOMO and next HOMO, the vinyl double bonds form bonding orbitals, and the single bonds linking the phenyl ring with the vinyl double bond are antibonding. In the LUMO, the vinyl double bonds are antibonding, and the single bonds are bonding. On the other hand, the next HOMO and next LUMO of the *trans*-**3** compound are localized on the benzene ring and the amplitude on vinyl double bond diminishes. These characters of MOs also explain the geometry changes in the excited states as mentioned above. The HOMO of the *trans*-**4** compound spreads over the oxygen lone pairs, which is the origin of the low-lying S_1 state in the *trans*-**4** compound.

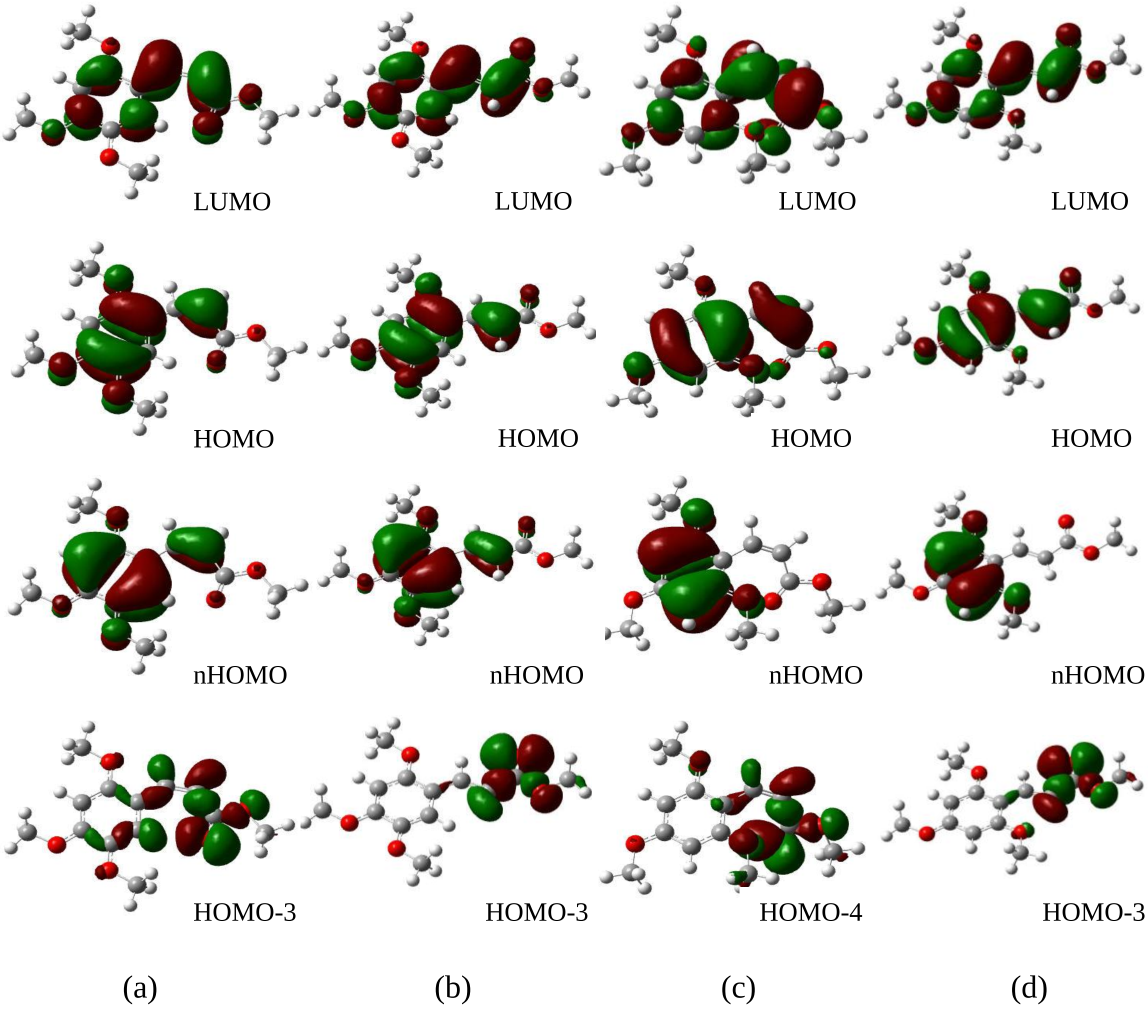

Figure 17 MOs relevant to the low-lying excited states for: (a) *cis*-**4**, (b) *trans*-**4**, (c) *cis*-**5**, and (d) *trans*-**5** of the trimethoxy substituted molecules.

The SAC-CI excitation spectra for the monomethoxy substituted molecules are compared with the experimental absorption spectra in Figure 18. The experimental spectra were observed in methanol, and the polar solvent effect in terms of the energy shift was small for the ortho- and meta-substitution (less than 4 nm), and nonnegligible for para-substitution (10-20 nm) from the experimental evidence.[7] The SAC-CI absorption spectrum of the *cis*-**3** substituted compound consists of a single absorption band, and that of the *trans*-**3** compound consists of closely separated two peaks, which is in good agreement with the experimental spectra. The absorption spectra of the ortho-(*cis*-**1** and *trans*-**1**) and meta-(*cis*-**2** and *trans*-**2**) substituted compounds consist of two distinct absorption bands. Compound **1** has two peaks with a large oscillator strength, whereas the spectra of compound **2** show a single strong peak in the higher energy region, with a shoulder on the lower energy side. These trends were well reproduced by the present SAC-CI calculations.

The SAC-CI and experimental spectra of the trimethoxy substituted compounds are compared in Figure 19. For the trimethoxy substituted compounds, the appearance of the SAC-CI absorption spectra of the *cis*-**4** and *trans*-**4** (ortho-, meta- and para-substituted) compounds was similar to those of the *cis*-**1** and *trans*-**1** (ortho-substituted) compounds, showing two distinct bands but with the lower peak having a higher intensity. This is in good agreement with the experimental measurements. The absorption of the compound **4** in the lower energy region may be useful for blocking of the UVA light In contrast, the absorption spectra of the *cis*-**5** and *trans*-**5** **(**ortho- and para-substituted) compounds resemble those of the *cis*-**3** and *trans*-**3** **(**para-substituted) compounds that show a single band with a small shoulder in the higher energy region. Our theory also reproduced these experimental data.

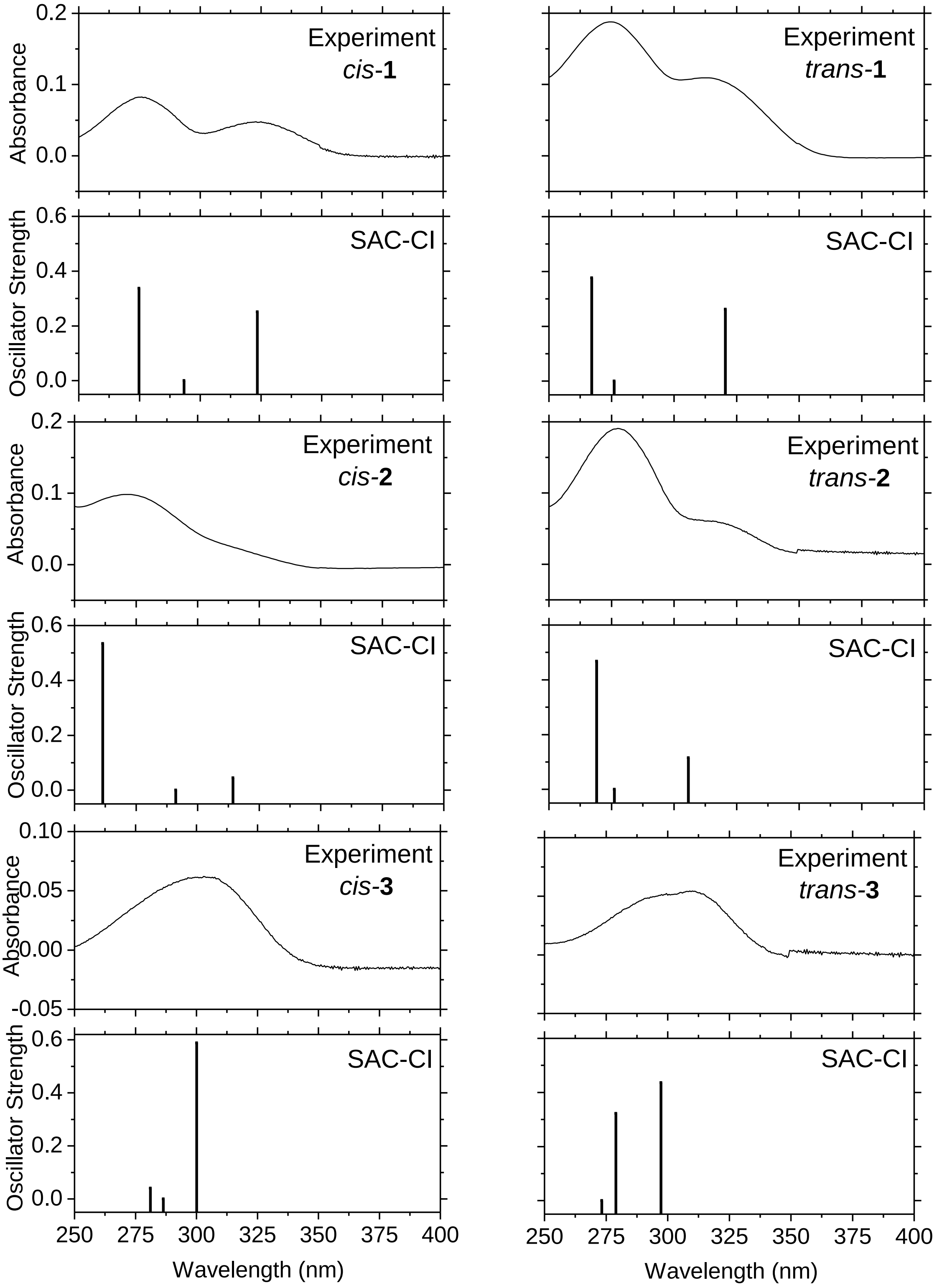

Figure 18 SAC-CI absorption spectra of the *cis*- and *trans*-isomers of the monomethoxy compounds compared with the experimental spectrum in methanol.

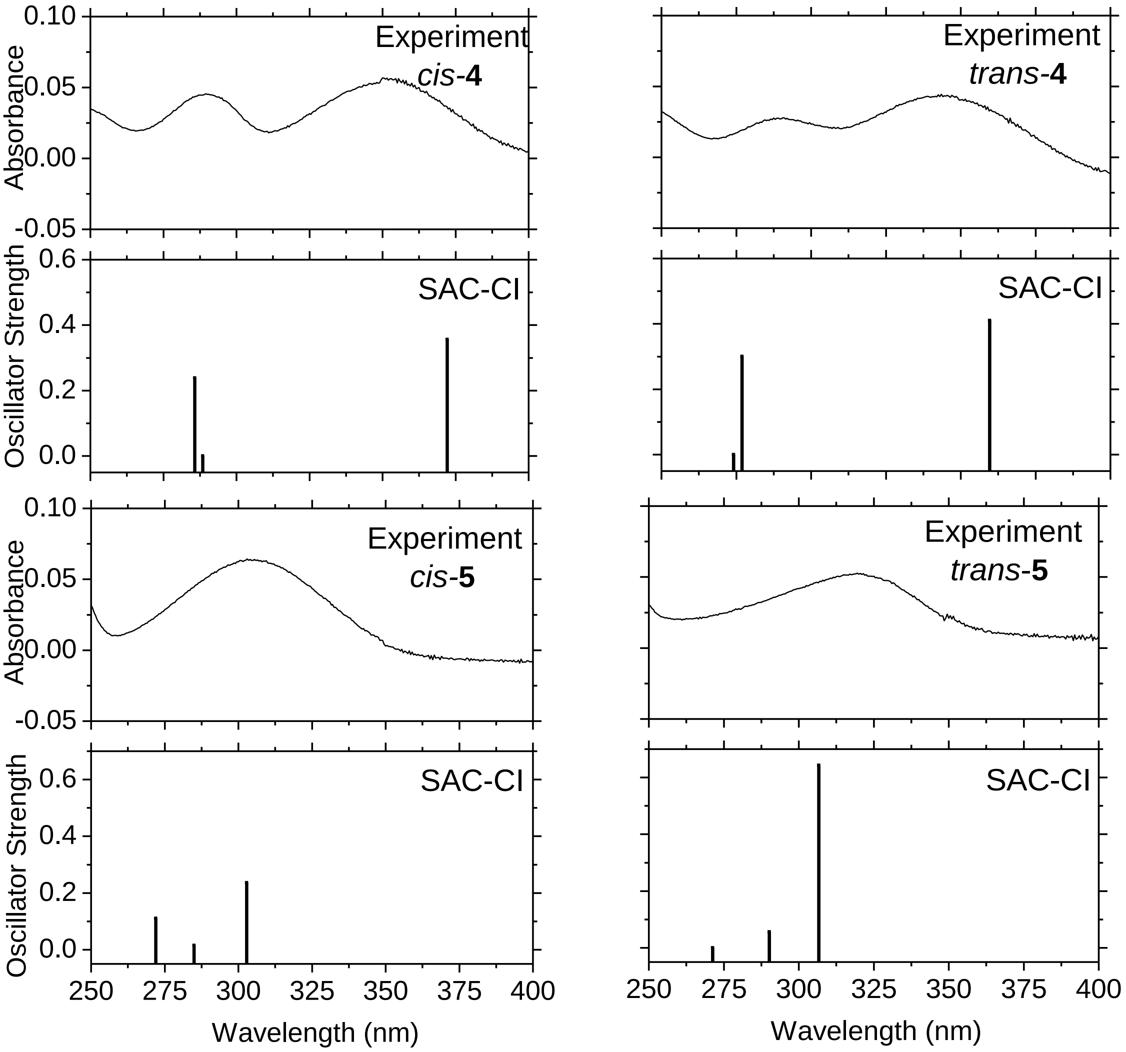

Figure 19 SAC-CI absorption spectra of the *cis*- and *trans*-isomers of the trimethoxy compounds compared with the experimental spectrum in methanol.

The experimental spectra show that the absorption intensity of the *trans*-isomers is larger than that of the corresponding *cis*-isomers in all the compounds. This indicates that the *trans*-isomers have better absorption efficiencies than the *cis*-isomers do. This trend was also reproduced by our SAC-CI calculations. In general, the transition dipole moment is determined by the transition dipole integrals and configuration interaction. In the present case, although the oscillator strength was distributed over two $1A'$ and $2A'$ from the configuration interaction, the difference between the *cis*- and *trans*-isomers could be attributed to the transition dipole integrals. The HOMO and LUMO orbitals of the *trans*-isomer are spread more broadly than those of the *cis*-isomer, which leads to the difference in the oscillator strength.

2.2.2 SAC-CI emission spectra

The emission energies of these molecules have also been calculated using the SAC-CI method. The stable geometries of the S_1 state were located using CIS followed by the SAC-CI calculations of the vertical emission energies. The calculated emission energies, oscillator strength, and Stokes shifts are compared with the experimental data in hexane and methanol solutions in Table 8. The dipole moment and excitation character of each excited state are also given in the same table.

Table 8 Excitation energy (E_{ex}), emission wavelength (λ_{max}), oscillator strength (f), excitation character and dipole moment for the *cis*- and *trans*-isomers of methoxy substituted cinnamates calculated by using the SAC-CI/D95(d) level of theory.

Molecule	State	E_{ex} (eV)	λ_{max} (nm)	f	Stokes shift (eV)	Excitation character	Dipole Moment (D) $\lvert\mu\rvert$[a]	Experiment (nm) MeOH	Hexane
cis-**1**	*1A′*	3.43	361	0.41	0.40	0.83 (H→L)	5.50 (3.15)	409	361
trans-**1**	*1A′*	3.37	367	0.44	0.50	0.85 (H→L)	4.68 (3.32)	405	359
cis-**2**	*1A′*	3.53	351	0.10	0.41	0.76 (H→L)	7.15 (1.48)	410	351
trans-**2**	*1A′*	3.62	343	0.29	0.44	0.84 (H→L)	5.74 (1.05)	409	350
cis-**3**	*1A′*	3.55	349	0.63	0.58	0.91 (H→L)	2.81 (1.63)	468	354
trans-**3**	*1A′*	3.52	352	0.61	0.65	0.90 (H→L)	4.89 (4.37)	462	351
cis-**4**	*1A′*	2.92	424	0.44	0.41	0.90 (H→L)	7.48 (3.48)	461	397
trans-**4**	*1A′*	3.04	408	0.51	0.41	0.90 (H→L)	7.19 (4.11)	461	398
trans-**5**	*1A′*	3.43	362	0.68	0.61	0.90 (H→L)	4.43 (6.04)	463	358

[a] Values in parentheses show the dipole moment of the ground state (*XA′*).

All the compounds, except for the *cis*-**5** compound, were calculated to have the local minima in the planar structure. The global minimum of the excited state is the conical intersection where the dihedral angle of the C_3-C_8-C_{10}-C_{12} chain is about 90°. Molecules excited to the S_1 state with sufficient energy relax through this conical intersection beyond an energy barrier to the ground state by nonradiative decay. Nonetheless, a weak emission was observed experimentally from this local minimum of the S_1 state in the coplanar structure, in particular for compound **2**. This emission from the local minimum of the S_1 state is discussed in this work. The bond distances in the S_1 state of these molecules are shown in Figure 10 and 11.

In general, the SAC-CI calculations reproduced the experimental trends observed in hexane solution satisfactorily. The emission energies of molecules were in the order of: compounds **2** and **3** (~350 nm) < compounds **1** and **5** (~360 nm) <

compound **4** (~400 nm). The deviation from the experimental values was within 10 nm, except for the *cis*-**4** compound. The transition was characterized as the HOMO-LUMO transition, and the SAC-CI coefficients are localized for this configuration. The calculated oscillator strengths were in the range 0.41-0.68 for all the molecules, except for compound **2**. As shown in the absorption data, the S_1 state of compound **2** also had a low oscillator strength in the ground state geometry, and the transition probability is distributed to the S_3 state. The calculated Stokes shifts were 0.40-0.50 eV for compounds **1**, **2**, and **4**, and these were slightly larger, 0.58-0.65 eV for compounds **3** and **5** where the para-position is substituted by a methoxy group. This means that the excited state geometry relaxations in the S_1 state of compounds **3** and **5** are larger than those for compounds **1**, **2**, and **4**.

A red shift was observed in methanol for all the compounds. To interpret this energy shift, the dipole moments of the S_0 and S_1 states calculated for the optimized geometry of the S_1 state are compared in Table 2. The calculated dipole moments in the excited state are larger than those in the ground state, which explains the experimental red shift qualitatively. The red shift of the emission in methanol was marked in compounds **3** and **5** (about 100 nm), for which our calculations could not explain this effect.

2.2.3 Relaxation processes

The relaxation processes in the excited states are important for the UVB blocking molecules. We examined the S_1 potential energy surface of *trans*-**2** and *trans*-**3** which mainly leads to decay by fluorescence and non-radiative decay through conical intersection, respectively.[7] Since the SAC-CI method is based on the single-reference theory, it is difficult to obtain the potential energy surface around the conical intersection. Then, we tried the CASSCF calculations but failed in the excited state optimization and even could not get convergence at the geometries of the large torsion angles. The CIS method is not reliable for these geometries. Therefore, we performed the SAC-CI partial optimization of the S_1 state for the torsion angles from 0 to 75 degrees with all the other coordinates being optimized. Because of the computational limitation, the small basis sets DZV [3s2p/2s] and restricted active space (7 occupied and 33 unoccupied MOs) were used and the perturbation selection of the operator was not performed in the SAC-CI calculations.

The potential energy curves along the minimum energy path of the S_1 state are shown for *trans*-**2** and *trans*-**3** in Fig. 11. In *trans*-**2**, the energy barrier to the conical intersection was calculated to be about 5.5 kcal/mol (0.24 eV), while *trans*-**3** has almost no energy barrier. These calculations qualitatively explain the experimental fact that the activation energies based on the non-radiative deactive rate of *trans*-**2** and *trans*-**3** compounds were estimated to be 1.4 and 0.4 kcal/mol, respectively.[7] The ground state surface of *trans*-**3** was too steep along the torsion, for which we think the errors come from the quasi-degenerate character of the states and the restricted active space.

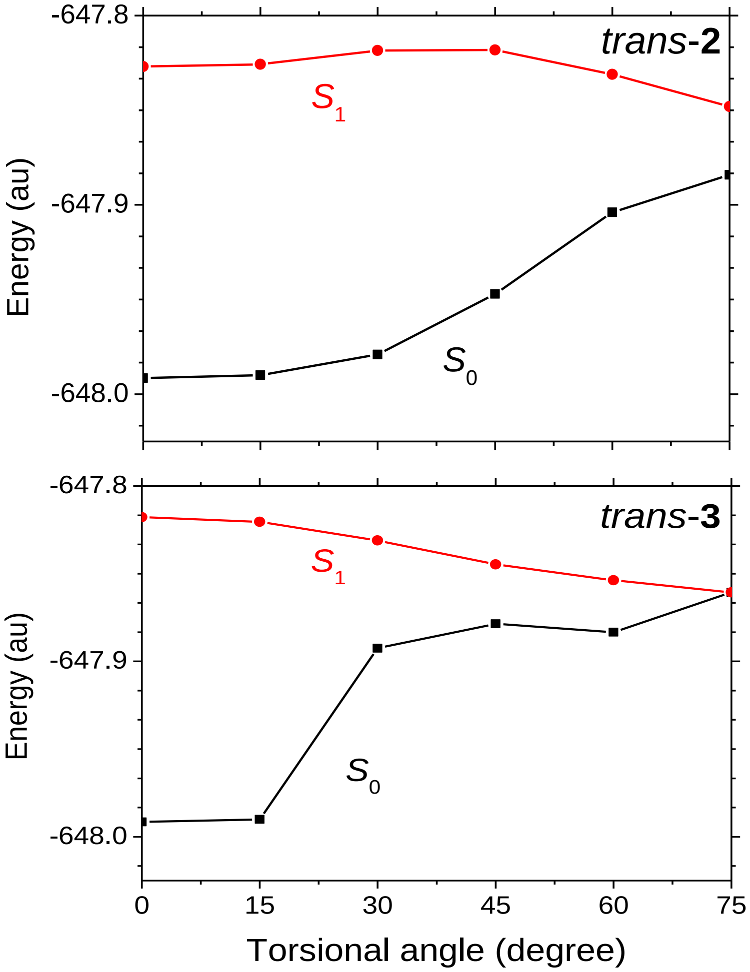

Figure 20 The SAC-CI potential energy curves along the minimum energy path of the S_1 state are shown for *trans*-**2** and *trans*-**3**. The SAC-CI calculations using DZV [3s2p/2s] and limited active space were performed without perturbation selection of operators.

3 Quantum Chemical Calculations

Previous study, the quantum chemical calculations of *cis*- and *trans*-isomer methoxy substituted cinnamate were performed by the semi-empircal (PM3) methods for ground state optimization and ZINDO methods for excited state energies and transition moments as implemented in the Hyperchem 5.1 program are given in Karpkird *et al.,* (2009).

Comparison of the excitation energy and oscillator strengths results for *cis*- and *trans*-isomer of the ortho-(**1**), meta-(**2**) and para-(**3**)-monomethoxy substituted compounds between the calculated with ZINDO, TD-DFT and SAC-CI methods are shown in Table 9, Table 2 and Table 4, respectively. From Table 9, the semi-empirical calculation predicts that the lowest excited state is of n*π** character for all character compound and that the next two higher excited states are of *ππ** character. It was found that the oscillator strengths of the n→π* transition is very weak comparing to the π→π* transition is much stronger. For the next two excited states as π→π* transition, indicates that the ortho-(**1**) and meta-(**2**) compounds have a weaker first and stronger second π→π* transition, whereas the para-(**3**) compound has a stronger first and weaker second π →π* transition.

Table 9 Calculated transition energies and oscillator strengths (*f*) for the monomethoxy cinnamates by using the ZINDO calculation.

Compounds	$S_0 \rightarrow S_1$ (n→π*)		$S_0 \rightarrow S_2$ (π→π*)		$S_0 \rightarrow S_3$ (π→π*)	
	(ν/cm^{-1})	*f*	(ν/cm^{-1})	*f*	(ν/cm^{-1})	*f*
cis-**1**	27400	0.00	33000	0.40	34600	0.23
trans-**1**	29800	0.00	33500	0.24	36000	0.67
cis-**2**	27500	0.00	32900	0.13	35500	0.46
trans-**2**	29600	0.00	34000	0.06	36700	0.80
cis-**3**	27600	0.00	32700	0.62	34800	0.01
trans-**3**	29700	0.00	34500	0.61	34800	0.35

The TD-B3LYP/6-31G(d) calculations for the gas phase based on the Table 4. For the monomethoxy substituted compounds found that the larger oscillator strengths of the ortho-(**1**) and meta-(**2**) positions are the transition from the ground state to the third excited state ($S_0 \rightarrow S_3$), whereas, the para-(**3**) position is the transition from the ground state to the first excited state ($S_0 \rightarrow S_1$).

The SAC-CI/D95(d) calculations also shown the A' states were assigned to the $\pi\pi^*$ excited states with a large oscillator strengths, while the A'' states were assigned to the $n\pi^*$ transition are displayed in Table 6. In the case of the ortho-(**1**) and meta-(**2**) compounds, the third excited state has the highest transition probability, whereas, the highest transition probability of the para-(**3**) compound was calculated for $S_0 \rightarrow S_1$ transition.

Therefore, the *cis*- and *trans*-isomer of the ortho-(**1**), meta-(**2**) and para-(**3**)-monomethoxy substituted compounds based on quantum chemical calculations by using the ZINDO, TD-DFT and SAC-CI methods provide that the similar results with the oscillator strengths and the transition.

CONCLUSIONS

The structural and electronic properties of cinnamate derivatives at five different substituted positions were investigated using the TD-DFT and SAC-CI methods. Both the *cis*- and *trans*-isomers were examined for ortho-(**1**), meta-(**2**), and para-(**3**)-monomethoxy and 2,4,5-(**4**) and 2,4,6-(**5**) trimethoxy substituted compounds.

All compounds have a local minimum in the *cis*- and *trans*-isomers in the planar structure in both the S_0 and S_1 states, except for the 2,4,6-trimethoxy compound. The SAC-CI/D95(d) calculations reproduced the recently observed absorption and emission spectra satisfactorily, and allowed a detailed assignment and interpretation of the spectra. Three low-lying excited states were found to be relevant for the absorption in the UV blocking energy region. The calculated oscillator strengths of the *trans*-isomers were larger than all the *cis*-isomers, which is in good agreement with experimental data. In the monomethoxy compounds at the ortho- and meta-positions, the most intense peak was assigned to the transition from the next HOMO to the LUMO, whereas in the para-compound it was assigned to the HOMO–LUMO transition. This feature was interpreted from the variation of the MOs due to the different substituted positions, and was used to explain the behavior of the excited states of the trimethoxy substituted compounds.

Quantum chemical calculations have provided reliable results and a useful insight into the optical properties of these molecules and therefore provide a useful tool for developing UVB blocking compounds with regard to the tuning of the absorption. High absorbance, broad absorption peak with small fluorescence quantum yield, and low radiative rate are expected for superior UVB sunscreen. Non-radiatve decay back to the initial ground-state is also relevant. Thus, the theoretical study of the relaxation process is important to design the superior UVB blocking molecules. In the present case, both *trans* and *cis*-forms can be generated in the course of the relaxation at around the conical intersection and *cis*-form also has absorption in the UVB region.

LITERATURE CITED

Becke, A.D. 1988. Density-functional exchange energy approximation with correct asymptotic behavior. **Phys. Rev. A** 38: 3098-3100.

Chakraborty, A., S. Kar and N. Guchhait. 2006. Photoinduced intramolecular charge transfer (ICT) reaction in trans-methyl p-(dimethylamino) cinnamate: A combined fluorescence measurement and quantum chemical calculations. **Chem. Phys.** 320: 75-83.

Chen, P.C. and Y.C. Chieh. 2003. Azobenzene and stilbene: a computational study. **J. Mol. Struct. (Theochem)** 624: 191-200.

Couteau, C., A. Faure, J. Fortin, E. Paparis and L. J.M. Coiffard. 2007. Study of the photostability of 18 sunscreens in creams by measuring the SPF in vitro. **J. Pharma. Biomed. Anal.** 44: 270-273.

Dunning T. H., Jr. and P. J. Hay. 1977. Gaussian Basis Sets for Molecular Calculations. **In Modern Theoretical Chemistry, Volume 3: Methods of Electronic Structure Theory,** Ed. H. F. Schaefer, III, Chap. 1. (Plenum Publishing Company, New York)

Ehara, M., P. Tomasello, J. Hasegawa and H. Nakatsuji. 1999. SAC-CI general-R study of the ionization spectrum of HCl. **Theor. Chem. Acc. Theor. Comput. Model. (Theor. Chim. Acta.)** 102: 161-164.

______, J. Hasegawa and H. Nakatsuji. 2005. SAC-CI Method applied to molecular spectroscopy, theory and applications of computational chemistry: The first 40 years, Ed. C. E. Dykstra, G. Frenking, K. S. Kim, and G. E. Scuseria (Elsevier, Oxford): 1099-1141.

Frisch, M.J., G.W. Trucks, H.B. Schlegel, G.E. Scuseria, M.A. Robb, J.R. Cheeseman, V.G. Zakrzewski, J.A. Montgomery, R.E., Jr. Stratmann, J.C. Burant, S. Dapprich, J.M. Millam, A.D. Daniels, K.N. Kudin, M.C. Strain, O. Farkas, J. Tomasi, V. Barone, M. Cossi, R. Cammi, B. Mennucci, C. Pomelli, C. Adamo, S. Clifford, J. Ochterski, G.A. Petersson, P.Y. Ayala, Q. Cui, K. Morokuma, D.K. Malick, A.D. Rabuck, K. Raghavachari, J.B. Foresman, J. Cioslowski, J.V. Ortiz, A. G. Baboul, B.B. Stefanov, G. Liu, A. Liashenko, P. Piskorz, I. Komaromi, R. Gomperts, R.L. Martin, D.J. Fox, T. Keith, M.A. Al-Laham, C.Y. Peng, A. Nanayakkara, M. Challacombe, P.M.W. Gill, B. Johnson, W. Chen, M.W. Wong, J.L. Andres, C. Gonzalez, M. Head-Gordon, E.S. Replogle and J. A. Pople. 1998, **GAUSSIAN98**. (Version A.1) Gaussian, Inc., Pittsburgh, PA.

Fujimoto K., J. Hasegawa, S. Hayashi, S. Kato and H. Nakatsuji. 2005. Mechanism of color-tuning in retinal proteins: SAC-CI and QM/MM study. **Chem. Phys. Lett.** 414: 239-242.

Fukuda, R. and H. Nakatsuji. 2008. Formulation and implementation of direct algorithm for the symmetry-adapted cluster and symmetry-adapted cluster-configuration interaction method. **J. Chem. Phys.** 128: 094105-094114.

Gagliardi, L., G. Orlandi, F. Bernardi, A. Cembran and M. Garavelli. 2004. A theoretical study of the lowest electronic states of azobenzene: the role of torsion coordinate in the *cis-trans* photoisomerization. **Theor. Chem. Acc.** 111: 363-372.

Groot de M., E. V. Gromov, H. Köppel and W. J. Buma. 2008. High-resolution spectroscopy of methyl 4-hydroxycinnamate and its hydrogen-bonded water complex. **J. Phys. Chem. B** 112: 4427-4434

Houari, S., A. Krallafa, F. Barbet, D. Bormann and B. Khelifa. 1999. Energetic considerations for the photoisomerization of vinyl cinnamates. **J. Comp. Mat. Sci.** 13: 270-275.

Huong, S.P., V. Andrieu, J. Reynier, E. Rocher and J. Fourneron. 2007. The photoisomerization of the sunscreen ethylhexyl-*p*-methoxycinnamate and its influence on the sun protection factor. **J. Photochem. Photobiol. A** 186: 65-70.

Ishida, M., K. Toyota, M. Ehara and H. Nakatsuji. 2001. Analytical energy gradients of the excited, ionized and electron-attached states calculated by the SAC-CI general-R method. **Chem. Phys. Lett.** 347: 493-498.

Jacquemin, D., E.A. Perpète, G. Scalmani, M.J. Frisch, I. Ciofini and C. Adamo. 2007. Fluorescence of 1,8-naphthalimide: A PCM-TD-DFT investigation. **Chem. Phys. Lett.** 448: 3-6.

______, ______, X. Assfeld, G. Scalmani, M.J. Frisch and C. Adamo. 2007. The geometries, absorption and fluorescence wavelengths of solvated fluorescent coumarins: A CIS and TD-DFT comparative study. **Chem. Phys. Lett.** 438:208-212.

Karpkird M. T., S. Pattanaargson, and B. Albinsson. 2009. Photophysical characterization of cinnmates. **Photochem. Photobiol. Sci.** DOI:10.1039/ B909695G

Krishnan, R., J.S. Binkley, R. Seeger and J.A. Pople. 1980. Self-consistent molecular orbital methods. XX. A basis set for correlated wave functions. **J. Chem. Phys.** 72: 650-654.

Lee, C., W. Yang and R.G. Parr. 1988. Development of the Colle-Salvetti correlation-energy formula into a functional of the electron density. **Phys. Rev. B** 37: 785-789.

Liao, H., Y. Lin, Y. Chou, F. Luo and B. wang. 2008. Theoretical study of optical and electronic properties of *p*-terphenyls containing cyano substituents as promising light-emitting materials. **J. Lumin.** 128: 1373-1378.

Meeto, W., S. Suramitr, S. Vannarat, S. Hannogngbua. 2008. Structural and electronic properties of poly(fluorene-vinylene) copolymer and its derivatives: Time-dependent density functional theory investigation. **Chem. Phys.** 349: 1-8.

Monhaphol, T., B. Albinsson, S.P. Wanichwecharungruang. 2007. 2-Ethylhexyl-2,4,5-tri methoxy cinnamate and di-(2-ethylhexyl)-2,4,5-trimethoxy-benzalmalonate as novel UVA filters. **J. Pharm. Pharmacol**, 59: 279-228.

Nakatsuji, H. 1978. Cluster expansion of the wavefunction. Excited states. **Chem. Phys. Lett.** 59: 362-364.

______, 1979. Cluster expansion of the wavefunction. Electron correlations in ground and excited states by SAC (symmetry-adapted-cluster) and SAC CI theories. **Chem. Phys. Lett.**67: 329-333.

______, 1979. Cluster expansion of the wavefunction. Calculation of electron correlations in ground and excited states by SAC and SAC CI theories. **Chem. Phys. Lett.** 67: 334-342.

______, and T. Koga. 1981. Force models for molecular geometry. **In The Force Concept in Chemistry",** Ed. by B. M. Deb, Chap.3: 137-217. (Van Nostrand Reinhold, New York).

______, 1983. Cluster expansion of the wavefunction, valence and rydberg excitations, ionizations, and inner-valence ionizations of CO2 and N2O studied by the sac and sac CI theories. **Chem. Phys.** 75: 425-441.

______, O. Kitao and T. Yonezawa. 1985. Cluster expansion of the wavefunction. valence and rydberg excitations and ionizations of pyrrole, furan, and cyclopentadiene. **J. Chem. Phys.** 83: 723-734.

______, 1992. Electronic structures of ground, excited, ionized and anion states studied by the SAC/SAC-CI theory. **Acta Chim. Acad. Sci. Hung.** 129: 719-776

Nakatsuji, H., J. Hasegawa and M. Hada. 1996. SAC-CI Study of the excited states of porphyrins. **J. Chem. Phys.** 104: 2321-2329.

______, ______, and K. Ohkawa. 1998. Excited states and electron transfer mechanism in the photosynthetic reaction cente of *Rhodopseudomonas Viridis*: SAC-CI study, **Chem. Phys. Lett.** 296: 499-504.

Oriol, L., M. Pi๑ol, J.L. Serrano and R.M. Tejedor. 2003. Synthesis, characterization and photoreactivity of liquid crystalline cinnamates. **J. Photochem. Photobiol. A-Chem.** 155: 37-45.

Pattanaargson, S., T. Munhapol, N. Hirunsupachot and P. Luangthongaram. 2004. Photoisomerization of octyl methoxycinnamate. **J. Photochem. Photobiol. A-Chem.** 161: 269-274.

_____, and P. Limphong. 2001. Stability of octyl methoxycinnamate and identification of its photo-degradation product. **Int. J. Cosmet. Sci.** 23: 151-158.

Poolmee, P., M. Ehara, S. Hannongbua and H. Nakatsuji. 2005. SAC-Cl theoretical investigation on electronic structure of fluorene-thiophene oligomers. **Polymer** 46: 6474-6481.

Saha, B., M. Ehara and H. Nakatsuji. 2007. Investigation of the electronic spectra and excited-state geometries of poly(*para*-phenylene vinylene) (PPV) and poly(para-phenylene) (PP) by the symmetry-adapted cluster configuration interaction (SAC-CI) method. **J. Phys. Chem. A** 111: 5473-5481.

Serpone, N., D. Dondi and A. Albini. 2007. Inorganic and organic UV filters: Their role and efficacy in sunscreens and suncare products. **Inorg. Chim. Acta.** 360: 794-802.

Singh, T.S., S. Mitra, A.K. Chandra, N. Tamai and S. Kar. 2008. A combined experimental and theoretical study on photoinduced intramolecular charge transfer in trans-ethyl *p*-(dimethylamino)cinamate. **J. Photochem. Photobiol. A: Chem.** 197: 295-305.

Suramitr, S., S. Hannongbua and P. Wolschann. 2007. Conformational analysis and electronic transition of carbazole-based oligomers as explained by density functional theory. **J. Mol. Struct. (Theochem)** 807: 109-119.

_____, T. Kerdcharoen, T. Srikhirin and S. Hannongbua. 2005. Electronic properties of alkosy derivativs of poly(*para*-phenylenevinylene), investigated by time-dependent density functional theory calculations. **Syn. Met.** 155: 27-34.

Smith, G.J. and I.J. Miller. 1998. The effect of molecular environment on the photochemistry of *p*-methoxycinnamic acid and its esters. **J. Photochem. Photobiol. A** 118: 93-97.

Wan, J., M. Ehara, M. Hada and H. Nakatsuji. 2000. Electronic excitation and ionization spectra of cyclopentadiene: Revisit by the symmetry-adapted cluster-configuration interaction method. **J. Chem. Phys.** 113: 5245-5252.

______, J. Meller, M. Hada, M. Ehara and H. Nakatsuji. 2000. Electronic excitation spectra of furan and pyrolle: Revisited by the symmetry-adapted cluster-configuration interaction method. **J. Chem. Phys.** 113: 7853-7866.

Wang H., B. Zhai, W. Tang, J. Yu and Q. Song. 2007. Photosensitized *Z-E* isomerization of cinnamate by covalently linked 2-(3',4'-dimenthoxybenzoyl) benzyl moiety via triplet-triplet energy transfer. **Chem. Phys.** 333: 229-235.

Wu C., S. Tretiak and V.Y. Chernyak. 2007. Excited states and optical response of a donor-acceptor substituted polyene: A TD-DFT study. **Chem. Phys. Lett.** 433: 305-311.

Yang, B., Z. Xie, H. Zhang, H. Xu, M. Hanif, X. Gu, F. He, J. Yu, Y. Ma, J. Shen, X. Liu, and J. Feng. 2008. Theoretical study of 2,5-diphenyl-1,4-distyrylbenzene (A model compound of PPV): A comparison of the electronic structure and photophysical properties of *cis*- and *trans*-isomers. **Chem. Phys.** 345: 23-31.

CURRICULUM VITAE

NAME : Miss Malinee Promkatkaew

BIRTH DATE : April 2, 1985

BIRTH PLACE : Chiang-Rai, THAILAND

NATIONALITY : Thai

EDUCATION :

YEAR	INSTITUTION	DEGREE/DIPLOMA
2007	Naresuan University	B.Sc. (Biology)

SCHOLASHIP : Postgraduate Education and Research Program in Petroleum, Petrochemical Technology and Advance Materials (NCE-PPAM) (2007-2008)

Thailand Graduate Institute of Science and Technology (TGIST) (2008-2009)

Teaching Assistance, Physical Chemistry Division, Kasetsart University (2008)

Bilateral Research Cooperation (BRC), Faculty of Science, Kasetsart University (2009)

PUBLICATIONS

1. Malinee Promkatkaew, Songwut Suramitr, Thitinun Karpkird Monhaphol, Supawadee Namuangruk, and Supa Hannongbua. **The Photophysical Properties of Structural and Electronic of Methoxy Subsitited 2-Ethylhexyl-Cinnamates, Based on Quantum Chemical Calculations.** The proceeding of 34th Congress on Science and Technology of Thailand (STT34). Queen Sirikit National Convention Center, Bangkok, Thailand, 31 October - 2 November 2008.

การศึกษาสมบัติฟิสิกส์เชิงแสงด้านโครงสร้างและอิเล็กทรอนิกส์ของอนุพันธ์ซินนาเมต โดยใช้การคำนวณทางเคมีควอนตัม

THE PHOTOPHYSICAL PROPERTIES OF STRUCTURAL AND ELECTRONIC OF METHOXY SUBSTITUTED 2–ETHYLHEXYL-CINNAMATES, BASED ON QUANTUM CHEMICAL CALCULATIONS

มาลินี พรหมขัติแก้ว[1,2], ทรงวุฒิ สุรมิตร[1,2*], ธิตินันท์ กาพย์เกิด หมั่นหาผล[1], สุภาวดี นาเมืองรักษ์[3] และ สุภา หารหนองบัว[1,2]

Malinee Promkatkaew[1,2], Songwut Suramitr[1,2], Thitinun Karpkird Monhaphol[1], Supawadee Namuangruk[3] and Supa Hannongbua[1,2]

[1]Department of Chemistry, Faculty of Science, Kasetsart University, Bangkok 10900, Thailand, [2]Center of Nanotechnology, Kasetsart University, Bangkok 10900, Thailand, [3]National Nanotechnology Center (NANOTEC), National Science and Technology Development Agency (NSTDA), 130 Paholyothin Rd., Klong 1, Klongluang, Pathumthani 12120, Thailand *E-mail: fsciswsm@ku.ac.th, Tel: +66-2-562-5555 Ext. 2227

บทคัดย่อ: งานวิจัยนี้ได้ใช้การคำนวณทางเคมีควอนตัม ศึกษาสมบัติฟิสิกส์เชิงแสงด้านโครงสร้างและอิเล็กทรอนิกส์ของอนุพันธ์ซินนาเมต ที่มีหมู่แทนที่ที่ตำแหน่งต่างกันห้าตำแหน่งบนวงเบนซีน ได้แก่ สารซินนาเมตที่มีหมู่เมธอกซีที่ตำแหน่งออร์โท-(1) เมตา-(2) พารา-(3) 2,4,5-(4) และ 2,4,6-(5) ทั้งแบบทรานซ์และซิสไอโซเมอร์ ผลการศึกษาทั้งในสภาวะพื้นและ สภาวะกระตุ้นพบว่า อนุพันธ์ของซินนาเมตทุกโมเลกุลสามารถดูดกลืนแสงยูวีได้ในช่วง 220 - 340 nm โดยผลที่ได้สอดคล้องกับการทดลอง ซึ่งพบว่าค่าความยาวคลื่นของการดูดกลืนแสงของโครงสร้างแบบทรานซ์มากกว่าซิสไอโซเมอร์ นอกจากนี้ยังพบว่าสารซินนาเมตที่มีหมู่เมทอกซี่แทนที่ที่ตำแหน่งออร์โท และ เมตา จะเกิดการกระตุ้นของอิเล็กตรอนจากระดับพลังงาน HOMO-1 ไปยัง LUMO ในขณะที่ตำแหน่งพาราจะเกิดการกระตุ้นของอิเล็กตรอนจากระดับพลังงาน HOMO ไปยัง LUMO

Abstract: The photophysical properties of five different substituted positions of 2-ethylhexyl-cinnamate derivatives were investigated based on quantum chemical calculations. This series includes *trans*- and *cis*-isomers of 2-ethylhexyl-ortho-(1), meta-(2), para-(3)-methoxycinnamtes, 2,4,5-(4) and 2,4,6-(5)-trimethoxycinnamates. Ground state geometries were calculated by the density functional theory (DFT) with B3LYP at 6-31G(d) and cc-pVDZ basis sets. Excitation energy calculations were analyzed by the time-dependent density functional theory (TD-DFT). All compounds absorb UVR radiation, which provide similar results to experimental data. The absorption wavelength (220-340 nm) of *trans*-isomers are higher than all *cis*- isomers. In addition, the electronic transition of cinnamates with methoxy substituted at ortho and meta positions correspond to the electronic excitation from HOMO-1 to LUMO. Whereas, those for para position correspond to the electronic excitation from HOMO to LUMO.

Introduction: The sun emits a wide spectrum of electromagnetic waves of which ultraviolet radiation (UVR) is the most aggressive towards cellular compounds. Solar UV radiation reaches the earth as well as our skin, is composed of 5-10% highly energetic UVB (290-320 nm) and 90-95% UVA (320-400 nm) which is less energetic, but penetrates the skin deeper. The UV radiations are harmful to the human skin. The interesting arylene system is cinnamate which is widely used as sunscreen agent, 2-ethylhexyl-para-methoxycinnamate as well as other cinnamate derivatives. In this work, the structural and electronic properties of *cis*- and *trans*-isomers of methoxy substituted 2-ethylhexyl-cinnamates-ortho-(1)-, meta-(2)-, para-(3)-methoxycinnamate, 2,4,5-(4) and 2,4,6-(5)-trimethoxycinnamates are shown in Table 1. All compounds were investigated by using quantum chemical calculation. In addition, the mono-substituted methoxycinnamates were used for explaining the behavior of tri-substituted methoxycinnamates. The obtained results will lead to the understanding of the UV absorption and emission properties between two isomers that can be used in cosmetics.

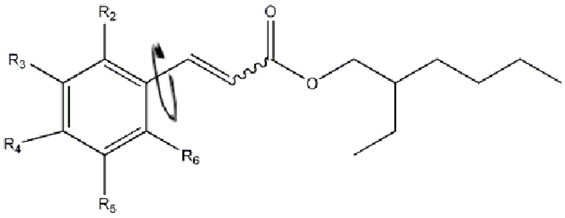

Table 1 Chemical structure of cinnamate derivatives

Compounds	R2	R3	R4	R5	R6
1	OCH_3	H	H	H	H
2	H	OCH_3	H	H	H
3	H	H	OCH_3	H	H
4	OCH_3	H	OCH_3	OCH_3	H
5	OCH_3	H	OCH_3	H	OCH_3

Methodology: The torsional energy curve of the *cis*- and *trans*-isomers of 10 compounds were investigated by partial optimization, based on the B3LYP/6-31G(d) and B3LYP/cc-pVDZ methods. All calculations were performed by the GAUSSIAN03 and TURBOMOLE suite of programs. The torsional angle (θ) is defined as the σ bond that can be rotated at θ = 0° corresponding to the *cis*-isomer and θ = 180° corresponding to the *trans*-isomer. Structures at various torsional angles (from θ = 0° to 180° in steps of 30°) were partially optimized. All stationary points located on the torsional energy were characterized as minima by harmonic frequency calculations (for minimum energy structures, all frequencies are real). Whereas, the vertical excitation energies were performed by single point calculations at the optimized ground state geometries by using TD-B3LYP/6-31G(d) and TD-B3LYP/cc-pVDZ calculations.

Results, Discussion and Conclusion: The structural results of the *cis*- and *trans*-isomers of methoxy substituted 2-ethylhexyl-ortho-(1)-, meta-(2)-, para-(3)-methoxycinnamte, 2,4,5-(4) and 2,4,6-(5)-trimethoxycinnamates. All compounds are stable at *cis*- and *trans*-isomers and the torsional angle locates at 0° and 180°, respectively (see Figure 1). An explanation is attributed by the intra-molecular hydrogen bonding between the hydrogen atom in the compounds and the oxygen atom that induces the geometry stabilization.

In Table 2 shows the excitation energy for mono-substituted methoxycinnamates. The largest transition probabilities of ortho- (*cis-1* and *trans-1*) and meta- (*cis-2* and *trans-2*) substituted methoxycinnamates are the transition from the ground state to the third excited state ($S_0 \rightarrow S_3$) and main electronic transitions are corresponding to HOMO-1 excite to LUMO.Whereas, the largest transition possibilities of para-substituted methoxycinnamates (*cis-3* and *trans-3*) is the transition from the ground state to the first excited state ($S_0 \rightarrow S_1$) and corresponding to the electronic excitation from HOMO to LUMO. Tri-methoxy substituted at ortho, meta and para positions (*cis-4* and *trans-4*) give the largest transition from ground state to first excited state ($S_0 \rightarrow S_1$). The main electronic transition is corresponded to HOMO excite to LUMO, as same as the compounds which have only substituted at ortho and para position (*cis-5* and *trans-5*). It is indicated that the para-methoxy substitution is an important effect to electronic properties of 2-ethylhexyl cinnamate (see Figure 1).

Table 2 Absorption wavelength (λ_{max}), oscillator strengths (*f*), and wave function composition (wf) for the singlet electronic states of methoxy substituted of 2-ethylhexyl-cinnamates calculated at TD-B3LYP/6-311G(d)//B3LYP/6-311G(d) and TD-B3LYP/cc-pVDZ//B3LYP/ cc-pVDZ level of theory.

Transition		λmax (nm)		*f*		wf	Expt.*
		6-31G(d)	cc-pVDZ	6-31G(d)	cc-pVDZ	6-31G(d) & cc-pVDZ	
cis-1	$S_0 \rightarrow S_1$	312.69	317.23	0.36	0.36	H → L 60%	313
	$S_0 \rightarrow S_3$	269.98	273.03	0.42	0.41	H-1 → L 58%	271
trans-1	$S_0 \rightarrow S_1$	321.41	325.20	0.28	0.28	H → L 60%	325
	$S_0 \rightarrow S_3$	279.71	281.78	0.39	0.39	H-1 → L 59%	276
cis-2	$S_0 \rightarrow S_1$	312.03	315.38	0.06	0.06	H → L 62%	313
	$S_0 \rightarrow S_3$	270.23	272.92	0.75	0.73	H-1 → L 57%	274
trans-2	$S_0 \rightarrow S_1$	330.14	333.30	0.04	0.04	H → L 65%	313
	$S_0 \rightarrow S_3$	275.84	277.94	0.66	0.66	H-1 → L 61%	278
cis-3	$S_0 \rightarrow S_1$	295.19	298.21	0.91	0.90	H → L 63%	303
trans-3	$S_0 \rightarrow S_1$	302.18	305.48	0.45	0.77	H → L 63%	309
cis-4	$S_0 \rightarrow S_1$	326.45	331.33	0.54	0.53	H → L 61%	345
	$S_0 \rightarrow S_3$	274.94	277.77	0.37	0.37	H-1 → L 60%	
trans-4	$S_0 \rightarrow S_1$	335.75	340.36	0.44	0.44	H → L 62%	349
	$S_0 \rightarrow S_3$	283.93	286.26	0.32	0.31	H-1 → L 62%	
cis-5	$S_0 \rightarrow S_1$	300.67	304.44	0.85	0.80	H → L 62%	305
trans-5	$S_0 \rightarrow S_1$	324.77	325.43	0.30	0.33	H → L 64%	320

* Adsorption spectra of cinnamates in methanol solution.

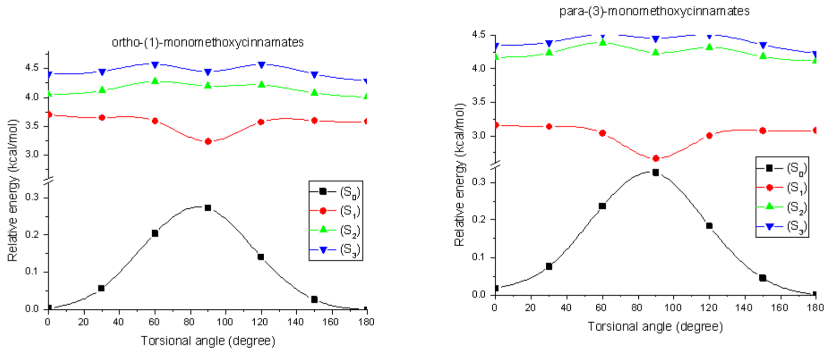

Figure 1 Torsional energy curves and excitation state of methoxy **substituted** at ortho-(1)-and para-(3)-methoxycinnamate derivatives as obtained by B3LYP/6-31G(d)

All compounds absorb UVR radiation, which provide similar results with experimental data. The absorption wavelength of *trans*-isomers are higher than all *cis*-isomers. The position of mono-methoxy substituted at ortho and meta position are corresponding to HOMO-1 excite to LUMO. Whereas, para position is corresponding to HOMO excite to LUMO and were used for explaining the behavior of tri-substituted 2,4,5 **(ortho, meta, para) and 2,4,6 (ortho, para)-**methoxycinnamates.

Acknowledgments: This work has been supported by the Thailand Research Fund and the Commission on Higher Education. MP is grateful to Thailand Graduate Institute of Science and Technology (TGIST) for a scholarship. The Postgraduate Education and Research Program in Petroleum, Petrochemical Technology and Advance Materials, the Center of Nanotechnology Kasetsart University, Kasetsart University Research and Development Institute (KURDI), National Nanotechnology Center (NANOTEC), Ministry of Science and Technology, Thailand are gratefully acknowledged for partial support and LCAC and computing center of KU for computing and research facilities.

Keywords: cinnamates, density functional theory, time-dependent density functional theory

References:

1. Monhaphol, T.; Albinsson, B.; Pattanaargson, S. *Pharmacy and Pharmacology*. **2007**, 59, 279-288.

2. Meeto, W.; Suramitr, S.; Vannarat, S.; Hannongbua, S. *Chemical Physics*, **2008**, 349, 1-8.

3. Suramitr, S.; Kerdcharoen, T.; Srikhirin, T.; Hannongbua, S. *Synthetic Metals*. **2005**, 155, 27-34.

4. Suramitr, S.; Hannongbua, S.; Wolschann, P.; *Journal of Molecular Structure: THEOCHEM*, **2007**, 807, 109-119.

2. Malinee Promkatkaew, Songwut Suramitr, Thitinun Karpkird Monhaphol, Supawadee Namuangruk, and Supa Hannongbua. **Photophysical Properties of Methoxy Substituted 2-Ethylhexyl-Cinnamates: A Quantum Chemical calculations.** The abstract of Pure and Applied Chemistry International Conference 2009 (PACCON2009), Naresuan University, Phitsanulok, Thailand, 14-16 January 2009.

Photophysical properties of methoxy substituted 2-ethylhexyl-cinnamates: A quantum chemical calculations

Malinee Promkatkaew[1,2], Songwut Suramitr[1,2], Thitinun Karpkird Monhaphol[1],
Supawadee Namuangruk[3] and Supa Hannongbua[1,2]

[1]*Department of Chemistry, Faculty of Science, Kasetsart University, Bangkok 10900, Thailand,*
[2]*Center of Nanotechnology, Kasetsart University, Bangkok 10900, Thailand,*
[3]*National Nanotechnology Center (NANOTEC), National Science and Technology Development Agency (NSTDA), 130 Paholyothin Rd., Klong 1, Klongluang, Pathumthani 12120, Thailand*
*E-mail; fsciswsm@ku.ac.th, Tel: +66-2-562-5555 ext 2227

The photophysical properties of five different substituted positions of 2-ethylhexyl-cinnamate derivatives were investigated based on quantum chemical calculations. This series includes *cis*- and *trans*-isomers of 2-ethylhexyl-ortho-(1), meta-(2), para-(3)-mono-methoxycinnamtes, 2,4,5-(4) and 2,4,6-(5)-tri-methoxycinnamates. Ground state geometries were calculated by the density functional theory (DFT) with B3LYP at 6-31G(d) and cc-pVDZ basis sets. Excitation energy calculations were analyzed by the time-dependent density functional theory (TD-DFT). The effects of solvent inclusion were analyzed by comparisons between gas-phase and methanol solution systems. All compounds absorb UVB radiation, which provide similar results to experimental data. The absorption wavelength (220-340 nm) of *trans*-isomers are higher than all *cis*-isomers. In addition, the electronic transition of 2-ethylhexyl-cinnamate with methoxy substituted at ortho and meta positions correspond to the electronic excitation from HOMO-1 to LUMO. Whereas, those for para position correspond to the electronic excitation from HOMO to LUMO.

REFERENCES

1. Chen, P.C.; Chieh. Y.C. *J. Mol. Struct. (Theochem).* **2003**, 624: 191-200.
2. Monhaphol, T.; Albinsson, B.; Pattanaargson, S. *J. Pharm. Pharmacol.* **2007**, 59, 279-288.
3. Meeto, W.; Suramitr, S.; Vannarat, S.; Hannongbua, S. *Chem. Phys.* **2008**, 349, 1-8.
4. Suramitr, S.; Hannongbua, S.; Wolschann, P. *J. Mol. Struct. (Theochem).* **2007**, 807, 109-119.

3. Malinee Promkatkaew, Songwut Suramitr, Thitinun Monhaphol Karpkird, Supawadee Namuangruk, Masahiro Ehara, and Supa Hannongbua. **Absorption and Emission Spectra of UVB Blocking Methoxy Substituted Cinnamates Investigated Using the Symmetry-Adapted Cluster Configuration Interaction Method.** The abstract of 13th Asian Chemical Congress (13ACC), Shanghai, China, 14-16 September 2009.

PT-OP38: Absorption and Emission Spectra of UVB Blocking Methoxy Substituted Cinnamates Investigated Using the Symmetry -Adapted Cluster Configuration Interaction Method

PROMKATKAEW Malinee[a,b], SURAMITR Songwut[a,b], KARPKIRD Monhaphol Thitinun[a,c], NAMUANGRUK Supawadee[d], EHARA Masahiro[c‡], and HANNONGBUA Supa[a,b*]

[a]Department of Chemistry, Faculty of Science, Kasetsart University, Bangkok 10900, Thailand
[b]Center of Nanotechnology, Kasetsart University, Bangkok 10900, Thailand
[c]Functional Compounds Special Research Unit (FCSRU), Kasetsart University, Bangkok 10900, Thailand
[d]National Nanotechnology Center (NANOTEC), 130 Klong 1, Klongluang, Phathumthani 12120, Thailand
[c]Institute for Molecular Science (IMS), 38 Myodaiji, Okazaki, 444-8585, Japan

The absorption and emission spectra of UVB blocking cinnamate derivatives with five different substituted positions were investigated using the symmetry-adapted cluster configuration interaction (SAC-CI) method. This series included *cis*- and *trans*-isomers of ortho-(**1**), meta-(**2**), and para-(**3**)-monomethoxy substituted compounds and 2,4,5-(**4**) and 2,4,6-(**5**)-trimethoxy compounds. The ground state and excited state geometries were obtained at the B3LYP/6-311G(d) and CIS/D95(d) levels of theory. All the compounds were stable as *cis*- and *trans*-isomers in the planar structure in both the S_0 and S_1 states, except the 2,4,6-trimethoxy compound. The SAC-CI/D95(d) calculations reproduced the recently observed absorption and emission spectra satisfactorily. Three low-lying excited states were found to be relevant for the absorption in the UV blocking energy region. The calculated oscillator strengths of the *trans*-isomers were larger than the respective *cis*-isomers, which is in good agreement with the experimental data. In the ortho- and meta-monomethoxy compounds, the most intense peak was assigned as the transition from next HOMO to LUMO, whereas in the para-monomethoxy compound, it was assigned to the HOMO to LUMO transition. This feature was used to explain the behavior of the excited states of the trimethoxy compounds. The emission from the local minimum in the planar structure was calculated for the *cis*- and *trans*-isomers of the five compounds. Our SAC-CI calculations provide reliable results and a useful insight into the optical properties of these molecules, and therefore, provide a useful tool for developing UVB blocking compounds.

Keywords: Cinnamate derivatives, Absorption, Emission, Electronic transition, SAC-CI

References

Pattanaargson, S., Munhapol, T., Hirunsupachot, N., Luangthongaram, P., **Photoisomerization of octyl methoxy cinnamate**, *J. Photochem. Photobiol. A.* **2004**, *161*, 269.

Poolmee, P., Ehara, M., Hannongbua, S., Nakatsuji, H., **SAC-CI theoretical investigation on electronic structure of fluorene-thiophene oligomers**, *Polymer,* **2005**, *46*, 6474.

Saha, B., Ehara, M., Nakatsuji, H., **Investigation of the electronic spectra and excited-state geometries of poly(para-phenylene vinylene) (PPV) and poly(para-phenylene) (PP) by the symmetry-adapted cluster configuration interaction (SAC-CI) method**. *J. Phys. Chem. A*, **2007**, *111*, 5473.

Corresponding author's Email, *fscisph@ku.ac.th Tel. +66-2-5625555 ext. 2140 Fax. +66-2-5793955
┴ehara@ims.ac.jp Tel. +81-564-55-7461 Fax. +81-564-55-7025

Project supported by the Thailand Research Fund (RTA5080005), Commission on Higher Education (CHE), Thailand Graduate Institute of Science and Technology (TGIST), Kasetsart University Research and Development Institute (KURDI), NCE-PPAM, Bilateral Research Cooperation (BRC) and Institute for Molecular Science (IMS).

4. Malinee Promkatkaew, Songwut Suramitr, Thitinun Monhaphol Karpkird, Supawadee Namuangruk, Masahiro Ehara, and Supa Hannongbua. **Absorption and Emission Spectra of UVB Blocking Methoxy Substituted Cinnamates Investigated Using the Symmetry-Adapted Cluster Configuration Interaction Method.** Journal of Chemical Physics.

PRESENTATION

Oral Presentation

1. Malinee Promkatkaew, Songwut Suramitr, Thitinun Karpkird Monhaphol, Supawadee Namuangruk, and Supa Hannongbua. **The Photophysical Properties of Structural and Electronic of Methoxy Subsitited 2-Ethylhexyl-Cinnamates, Based on Quantum Chemical Calculations.** The 34th Congress on Science and Technology of Thailand (STT34). Queen Sirikit National Convention Center, Bangkok, Thailand, 31October - 2 November 2008.

2. Malinee Promkatkaew, Songwut Suramitr, Thitinun Monhaphol Karpkird, Supawadee Namuangruk, Masahiro Ehara, and Supa Hannongbua. **Absorption and Emission Spectra of UVB Blocking Methoxy Substituted Cinnamates Investigated Using the Symmetry-Adapted Cluster Configuration Interaction Method.** The 13th Asian Chemical Congress (13ACC), Shanghai, China, 14-16 September 2009.

Poster Presentation

Malinee Promkatkaew, Songwut Suramitr, Thitinun Karpkird Monhaphol, Supawadee Namuangruk, and Supa Hannongbua. **Photophysical Properties of Methoxy Substituted 2-Ethylhexyl-Cinnamates: A Quantum Chemical calculations.** The Pure and Applied Chemistry International Conference 2009 (PACCON2009), Naresuan University, Phitsanulok, Thailand, 14-16 January 2009.

Photophysical Properties of Methoxy Substituted 2-Ethylhexyl-Cinnamates: A Quantum Chemical Calculations

Malinee Promkatkaew[1,2], Songwut Suramitr[1,2*], Thitinun Karpkird Monhaphol[1,3], Supawadee Namuangruk[4] and Supa Hannongbua[1,2]
[1]Department of Chemistry, Faculty of Science, Kasetsart University, Bangkok 10900, Thailand
[2]Center of Nanotechnology, Kasetsart University, Bangkok 10900, Thailand
[3]Functional Compounds Special Research Unit (FCSRU), Kasetsart University, Bangkok 10900, Thailand
[4]National Nanotechnology Center (NANOTEC), National Science and Technology Development Agency (NSTDA), Pathumthani 12120, Thailand
*Co-responding author: Tel. +66-2-562-5555 ext 2227, E-mail: fsciswsm@ku.ac.th

Introduction:

The sun emits a wide spectrum of electromagnetic waves of which ultraviolet radiation (UV) is the most aggressive towards cellular compounds. Solar UV radiation reaches the earth as well as our skin, is composed of 5-10% highly energetic UVB (290-320 nm) and 90-95% UVA (320-400 nm) which is less energetic, but penetrates the skin deeper. The UV radiations are harmful to the human skin. The interesting arylene system is cinnamate which is widely used as sunscreen agent, 2-ethylhexyl-para-methoxycinnamate as well as other cinnamate derivatives. In this work, the photophysical properties of *cis*- and *trans*-isomers of methoxy substituted 2-ethylhexylcinnamates-ortho-(1)-, meta-(2)-, para-(3)-methoxy-cinnamates, 2,4,5-(4) and 2,4,6-(5)-tri-methoxy-cinnamates are shown in Table 1. All compounds were investigated by using quantum chemical calculation. The obtained results will lead to the understanding of the UV absorption and emission properties between two isomers that can be used in cosmetics.

Table 1 Chemical structure of cinnamate derivatives.

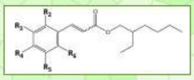

compounds	R_2	R_3	R_4	R_5	R_6
1	OCH_3	H	H	H	H
2	H	OCH_3	H	H	H
3	H	H	OCH_3	H	H
4	CH_3	H	CH_3	OCH_3	H
5	CH_3	H	CH_3	H	OCH_3

Methodology:

Ground state geometries of the *cis*- and *trans*-isomers of 5 compounds were calculated by full optimization, based on the HF/6-31G(d,p) and B3LYP/6-31G(d,p) methods. All calculations were performed by the GAUSSIAN03 suite of programs. The torsional angle (θ) is defined as the σ bond that can be rotated at θ = 0° corresponding to the *cis*-isomer and θ = 180° corresponding to the *trans*-isomer. Whereas, the vertical excitation energies were performed by single point calculations at the optimized ground state geometries by using TD-B3LYP/6-31G(d,p) calculations. The effects of solvent inclusion were analyzed by the conductor-like polarized continuum model (CPCM) in methanol solution systems.

Table 2 Absorption wavelength (*λmax*), oscillator strengths (*f*) and wavefunction composition for the singlet electronic states of *cis*- and of *trans*-isomer of methoxy substituted 2-ethylhexyl-cinnamates by using TD-B3LYP/6-31G(d,p)//HF/6-31G(d,p) and TD-B3LYP/6-31G(d,p)//B3LYP/6-31G(d,p)

Electronic Transition		TD-B3LYP/6-31G(d,p)//HF/6-31G(d,p)				TD-B3LYP/6-31G(d,p)//B3LYP/6-31G(d,p)				Wavefunction composition	Exp.*
		Gas phase		Solvent phase		Gas phase		Solvent phase			
		λ (nm)	*f*	λ (nm)	*f*	λ (nm)	*f*	λ (nm)	*f*		
cis 1	$S_0 \rightarrow S_1$	304	0.200	313	0.244	322	0.278	335	0.353	H → L (60%)	313
	$S_0 \rightarrow S_3$	252	0.201	251	0.171	280	0.382	282	0.038	H-1 → L (58%)	271
trans 1	$S_0 \rightarrow S_1$	300	0.296	315	0.341	313	0.360	330	0.413	H → L (60%)	325
	$S_0 \rightarrow S_3$	257	0.373	256	0.034	271	0.409	270	0.000	H-1 → L (59%)	276
cis 2	$S_0 \rightarrow S_1$	315	0.038	315	0.051	331	0.037	333	0.050	H → L (65%)	313
	$S_0 \rightarrow S_3$	260	0.455	261	0.278	276	0.666	281	0.000	H-1 → L (61%)	274
trans 2	$S_0 \rightarrow S_1$	301	0.055	312	0.079	312	0.059	324	0.087	H → L (62%)	313
	$S_0 \rightarrow S_3$	260	0.685	258	0.000	271	0.740	269	0.000	H-1 → L (57%)	278
cis 3	$S_0 \rightarrow S_1$	291	0.742	301	0.823	304	0.762	315	0.843	H → L (63%)	303
trans 3	$S_0 \rightarrow S_1$	285	0.856	299	0.953	296	0.897	311	0.995	H → L (63%)	309
cis 4	$S_0 \rightarrow S_1$	349	0.219	355	0.269	366	0.285	376	0.353	H → L (63%)	345
trans 4	$S_0 \rightarrow S_1$	334	0.322	351	0.359	345	0.386	365	0.430	H → L (62%)	349
cis 5	$S_0 \rightarrow S_1$	318	0.211	325	0.252	325	0.292	335	0.347	H → L (64%)	305
trans 5	$S_0 \rightarrow S_1$	291	0.801	300	0.850	301	0.835	312	0.873	H → L (62%)	320

* Absorption spectra of cinnamates in methanol solution

Results and Discussion:

cis-1 *cis-2* *cis-3* *cis-4* *cis-5*

Figure 1 Schmatic representation of intra-molecular H-bond interaction in *cis*-isomer of methoxy substituted 2-ethylhexyl-cinnamates, obtained from full optimization by B3LYP/6-31G(d,p).

trans-1 *trans-2* *trans-3* *trans-4* *trans-5*

Figure 2 Schmatic representation of intra-molecular H-bond interaction in *trans*-isomer of methoxy substituted 2-ethylhexyl-cinnamates, obtained from full optimization by B3LYP/6-31G(d,p).

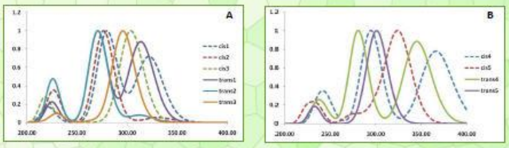

Figure 3 Absorption of *cis*- and *trans*-isomer of mono-(A) and tri-(B)-methoxy substituted 2-ethylhexyl-cinnamates by using TD-B3LYP/6-31G(d,p)//B3LYP/6-31G(d,p)

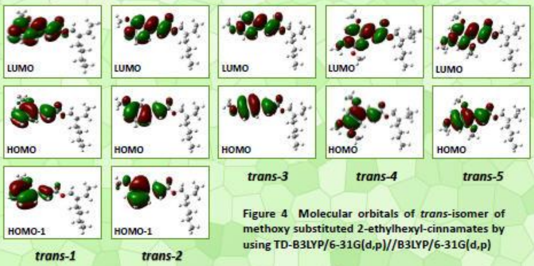

trans-3 *trans-4* *trans-5*

trans-1 *trans-2*

Figure 4 Molecular orbitals of *trans*-isomer of methoxy substituted 2-ethylhexyl-cinnamates by using TD-B3LYP/6-31G(d,p)//B3LYP/6-31G(d,p)

Conclusions:

All compounds absorb UVB radiation, which provide similar results with experimental data. The oscillator strengths of *trans*-isomers are higher than all *cis*- isomers. The position of mono-methoxy substituted at ortho and meta position are corresponding to HOMO-1 excite to LUMO. Whereas, para position is corresponding to HOMO excite to LUMO and were used for explaining the behavior of tri-substituted 2,4,5 (ortho, meta, para) and 2,4,6 (ortho, para)-methoxycinnamates.

References:

1. Chen, P.C.; Chieh. Y.C. *J. Mol. Struct. (Theochem)*. 2003, 624: 191-200.
2. Monhaphol, T.; Albinsson, B.; Pattanaargson, S. *J. Pharm. Pharmacol*. 2007, 59, 279-288.
3. Meeto, W.; Suramitr, S.; Vannarat, S.; Hannongbua, S. *Chem. Phys.* 2008, 349, 1-8.
4. Suramitr, S.; Hannongbua, S.; Wolschann, P. *J. Mol. Struct. (Theochem)*. 2007, 807, 109-119.

Acknowledgments:

This work has been supported by the Thailand Research Fund (TRF) and the Commission on Higher Education (CHE). MP is grateful to Thailand Graduate Institute of Science and Technology (TGIST) for a scholarship. The Postgraduate Education and Research Program in Petroleum, Petrochemical Technology and Advance Materials, the Center of Nanotechnology Kasetsart University, Kasetsart University Research and Development Institute (KURDI), National Nanotechnology Center (NANOTEC), Ministry of Science and Technology, Thailand are gratefully acknowledged for partial support and LCAC and computing center of KU for computing and research facilities.